

Dimension reduction in stochastic analysis of coupled systems

M. Arnst^{1,2*}, R. Ghanem¹, E. Phipps³ and J. Red-Horse³

¹ 210 KAP Hall, University of Southern California, Los Angeles, CA 90089, USA

² B52/3, Université de Liège, Chemin des Chevreuils 1, B-4000 Liège, Belgium

³ Sandia National Laboratories[†], P.O. Box 5800, Albuquerque, NM 87185, USA

SUMMARY

Coupled models with multiple physics, scales and/or domains arise in numerous areas of science and engineering. A key challenge in the formulation and implementation of coupled models is in facilitating the communication of information across physics, scale and/or domain interfaces. In a probabilistic context, any information that is communicated between model components is described in a statistical manner and requires an adapted probabilistic representation. While the number of sources of uncertainty can be expected to be large in many coupled problems, our contention is that exchanged statistical information often resides in a much lower dimensional space. In this work, we thus investigate the use of dimension-reduction techniques for the representation of exchanged information. We describe an adaptation of the Karhunen-Loeve decomposition to represent information as it is passed from component to component in a stochastic coupled model. The range of validity of the proposed dimension reduction is demonstrated on a stochastic multi-physics problem relevant to nuclear reactors. Copyright © 2000 John Wiley & Sons, Ltd.

KEY WORDS: uncertainty quantification, coupled systems, multi-physics, polynomial chaos

1. Introduction

The modeling and simulation of coupled systems governed by multiple physical processes that may exist simultaneously across multiple scales and domains represent critical tools for addressing numerous science and engineering challenges. However, models are by definition only approximations of their target scenarios, and are thus prone to modeling errors; also, parametric uncertainties exist as a reflection of limitations in experimental methods. Uncertainty Quantification (UQ) thus constitutes a key requirement for predictive simulations of coupled systems to find useful applications in supporting scientific discovery and engineering.

The probability theory provides a rigorous framework for UQ, which permits a unified treatment of modeling errors and parametric uncertainties. The first step in a probabilistic

*Correspondence to: 210 KAP Hall, University of Southern California, Los Angeles, CA 90089, USA

[†]Sandia National Laboratories is a multi-program laboratory managed and operated by Sandia Corporation, a wholly owned subsidiary of Lockheed Martin Corporation, for the U.S. Department of Energy's National Nuclear Security Administration under contract DE-AC04-94AL85000.

UQ analysis typically consists in using [1–3] methods from mathematical statistics [4, 5] to characterize the uncertain features of a simulation as random variables, fields, matrices, and/or operators. The second step then involves propagating the probability distribution of the inputs to a probability distribution of the predictions. This can be achieved by either Monte Carlo sampling techniques [6], or stochastic expansion methods. The latter typically involve the computation of a representation of the predictions as a Polynomial Chaos (PC) expansion. Several procedures are available to calculate the coefficients in this expansion, including embedded projection [7, 8], non-intrusive projection [8], and collocation [9–13].

A key challenge in the formulation and implementation of coupled models is in facilitating the communication of information across physics, scale or domain interfaces. This information can include that of physical properties, energetic quantities, or patches of solutions, among other quantities. While the number of sources of uncertainty can be expected to be large in many coupled problems, our contention is that exchanged information often resides in a much lower dimensional space. The exchanged information can, *a priori*, be expected to exhibit a *low effective stochastic dimension* in multi-physics problems when that information consists of a solution field that has been smoothed by a forward operator, and in multi-scale problems when it is obtained by summarizing a fine-scale quantity into a coarse-scale representation.

In this work, we investigate the use of dimension-reduction techniques for the representation of exchanged information. Specifically, we propose to represent information by an adaptation of the Karhunen-Loeve (KL) decomposition as it is passed from model component to model component. When the exchanged information indeed has a low effective stochastic dimension, this representation allows for a reduction in the requisite stochastic degrees of freedom to be achieved, while maintaining accuracy. We note that several references in the literature have already demonstrated the integration of dimension reduction in algorithms for solving stochastic partial differential equations, see, for instance, [14–20]; however, our contribution lies in highlighting the role that dimension reduction can play for coupled problems.

The outline of this paper is as follows. First, Sec. 2 outlines the methodology to be followed. Then, Sec. 3 describes an adaptation of the KL decomposition, which is well-adapted to construct a reduced-dimensional representation of information as it is passed from component to component in a stochastic coupled model. Subsequently, Sec. 4 provides details to assist the reader in implementing the framework. Finally, Secs. 5 and 6 demonstrate the proposed dimension reduction on an illustration problem, and provide numerical results.

2. Dimension reduction in stochastic analysis of coupled systems

We will now describe the methodology proposed to accommodate dimension reduction in algorithms for the solution of stochastic coupled models.

2.1. Deterministic problem

Consider a coupled system of two models:

$$\mathbf{f}_1(\mathbf{u}_1, \mathbf{q}_2) = \mathbf{0}, \quad \mathbf{u}_1 \in U_1, \quad \mathbf{q}_1 = \mathbf{g}_1(\mathbf{u}_1) \in Q_1, \quad (1)$$

$$\mathbf{f}_2(\mathbf{q}_1, \mathbf{u}_2) = \mathbf{0}, \quad \mathbf{u}_2 \in U_2, \quad \mathbf{q}_2 = \mathbf{g}_2(\mathbf{u}_2) \in Q_2. \quad (2)$$

We assume that each model component represents a well-posed single-physics, single-scale or single-domain problem: we assume that the first equation can be solved for \mathbf{u}_1 for a given \mathbf{q}_2 ,

and that the second equation can be solved for \mathbf{u}_2 for a given \mathbf{q}_1 . The system (1)-(2) is a general "two-way" coupled system that involves the transfer of information in both directions: the first equation depends on a quantity \mathbf{q}_2 that is a function of the solution \mathbf{u}_2 of the second equation, and the second equation depends, in turn, on a quantity \mathbf{q}_1 that is function of the solution \mathbf{u}_1 of the first equation. We assume that \mathbf{u}_1 and \mathbf{u}_2 , and \mathbf{q}_1 and \mathbf{q}_2 , are scalars, vectors, matrices or functions that take their values in Hilbert spaces U_1 and U_2 , and Q_1 and Q_2 .

2.2. Stochastic problem

Let the data (coefficients and/or loadings) of the first model component depend on a finite number of uncertain real parameters ξ_1, \dots, ξ_N . Let the only uncertainties that affect the second model component be those that are introduced in the first component and enter the second component through the coupling. Let the *sources of uncertainty* $\boldsymbol{\xi} = (\xi_1, \dots, \xi_N)$ be characterized by a probability distribution $P_{\boldsymbol{\xi}}$ on \mathbb{R}^N . Using a self-explanatory terminology, we call the sources of uncertainty $\boldsymbol{\xi}$ *internal* to the first model component, and *exogenous* to the second component. The stochastic model thus obtained consists in finding random variables \mathbf{u}_1 and \mathbf{u}_2 defined on the probability space $(\mathbb{R}^N, \mathcal{B}(\mathbb{R}^N), P_{\boldsymbol{\xi}})$ with values in U_1 and U_2 such that:

$$\mathbf{f}_1(\mathbf{u}_1(\boldsymbol{\xi}), \mathbf{q}_2(\boldsymbol{\xi}), \boldsymbol{\xi}) = \mathbf{0}, \quad \mathbf{u}_1(\boldsymbol{\xi}) \in U_1, \quad \mathbf{q}_1(\boldsymbol{\xi}) = \mathbf{g}_1(\mathbf{u}_1(\boldsymbol{\xi}), \boldsymbol{\xi}) \in Q_1, \quad P_{\boldsymbol{\xi}}\text{-a.s.}, \quad (3)$$

$$\mathbf{f}_2(\mathbf{q}_1(\boldsymbol{\xi}), \mathbf{u}_2(\boldsymbol{\xi})) = \mathbf{0}, \quad \mathbf{u}_2(\boldsymbol{\xi}) \in U_2, \quad \mathbf{q}_2(\boldsymbol{\xi}) = \mathbf{g}_2(\mathbf{u}_2(\boldsymbol{\xi})) \in Q_2, \quad P_{\boldsymbol{\xi}}\text{-a.s.} \quad (4)$$

2.3. Elementary implementation

Problem (3)-(4) can be discretized by either sampling-based techniques or stochastic expansion methods. The discretized coupled system of equations can then be solved by weakly-coupled successive-substitution approaches such as Jacobi or Gauss-Seidel iteration, or by strongly-coupled Newton iteration. A key advantage of successive-substitution approaches is that they enable the reuse of legacy codes already available for the solution of separate model components. Our point of departure, for this paper, is Algorithm 1, which involves the use of a stochastic expansion method and a Gauss-Seidel successive-substitution iterative scheme.

Given an initial representation of \mathbf{q}_2 , Algo. 1 starts out by solving the first component for a PC expansion of \mathbf{u}_1 and \mathbf{q}_1 in terms of the sources of uncertainty $\boldsymbol{\xi}$. Then, the expansion of \mathbf{q}_1 is passed to the second component, which is solved, in turn, for a PC expansion of \mathbf{u}_2 and \mathbf{q}_2 in terms of the $\boldsymbol{\xi}$. Subsequently, the updated expansion of \mathbf{q}_2 is passed to the first component, after which the whole procedure is repeated until convergence.

2.4. Implementation with dimension reduction

Algorithm 2 highlights the manner in which we propose to accommodate dimension reduction in algorithms for the solution of stochastic coupled models: information is represented by a truncated KL decomposition as it is communicated from the model component for which the sources of uncertainty are internal to the model component for which they are exogenous.

We say that the exchanged information has a low *effective stochastic dimension* when the KL decomposition is able to extract a low-dimensional representation of the exchanged information, that is to say when a truncated KL decomposition that only retains a small number of terms allows for the accurate representation of the information that crosses the

```

Input : initialization;
while (not converged) do
   $\ell = \ell + 1$ ;
  first subproblem
  | Solve  $\mathbf{f}_1(\star, \mathbf{q}_2^{(\ell-1)}(\boldsymbol{\xi}), \boldsymbol{\xi}) = \mathbf{0}$  for  $\mathbf{u}_1^{(\ell)}(\boldsymbol{\xi}) = \sum_{\alpha} \mathbf{u}_{1\alpha}^{(\ell)} H_{\alpha}(\boldsymbol{\xi})$ ;
  | Compute  $\mathbf{q}_1^{(\ell)}(\boldsymbol{\xi}) = \sum_{\alpha} \mathbf{q}_{1\alpha}^{(\ell)} H_{\alpha}(\boldsymbol{\xi})$ ;
  end
  second subproblem
  | Solve  $\mathbf{f}_2(\mathbf{q}_1^{(\ell)}(\boldsymbol{\xi}), \star) = \mathbf{0}$  for  $\mathbf{u}_2^{(\ell)}(\boldsymbol{\xi}) = \sum_{\alpha} \mathbf{u}_{2\alpha}^{(\ell)} H_{\alpha}(\boldsymbol{\xi})$ ;
  | Compute  $\mathbf{q}_2^{(\ell)}(\boldsymbol{\xi}) = \sum_{\alpha} \mathbf{q}_{2\alpha}^{(\ell)} H_{\alpha}(\boldsymbol{\xi})$ ;
  end
end

```

Algorithm 1: Elementary implementation.

```

Input : initialization;
while (not converged) do
   $\ell = \ell + 1$ ;
  first subproblem
  | Solve  $\mathbf{f}_1(\star, \hat{\mathbf{q}}_2^{(\ell-1)}(\boldsymbol{\xi}), \boldsymbol{\xi}) = \mathbf{0}$  for  $\hat{\mathbf{u}}_1^{(\ell)}(\boldsymbol{\xi}) = \sum_{\alpha} \hat{\mathbf{u}}_{1\alpha}^{(\ell)} H_{\alpha}(\boldsymbol{\xi})$ ;
  | Compute  $\hat{\mathbf{q}}_1^{(\ell)}(\boldsymbol{\xi}) = \sum_{\alpha} \hat{\mathbf{q}}_{1\alpha}^{(\ell)} H_{\alpha}(\boldsymbol{\xi})$ ;
  end
  hand-shaking region
  | Approximate  $\hat{\mathbf{q}}_1^{(\ell)}(\boldsymbol{\xi})$  by KL  $\hat{\mathbf{q}}_1^{n(\ell)}(\boldsymbol{\eta}^{(\ell)} \boldsymbol{\xi}) = \bar{\mathbf{q}}_1^{(\ell)} + \sum_{i=1}^n \sqrt{\lambda_i^{(\ell)}} \boldsymbol{\varphi}_i^{(\ell)} \eta_i^{(\ell)}(\boldsymbol{\xi})$ ;
  end
  second subproblem
  | Solve  $\mathbf{f}_2(\hat{\mathbf{q}}_1^{n(\ell)}(\boldsymbol{\eta}^{(\ell)}(\boldsymbol{\xi})), \star) = \mathbf{0}$  for  $\hat{\mathbf{u}}_2^{(\ell)}(\boldsymbol{\xi}) = \sum_{\alpha} \hat{\mathbf{u}}_{2\alpha}^{(\ell)} H_{\alpha}(\boldsymbol{\xi})$ ;
  | Compute  $\hat{\mathbf{q}}_2^{(\ell)}(\boldsymbol{\xi}) = \sum_{\alpha} \hat{\mathbf{q}}_{2\alpha}^{(\ell)} H_{\alpha}(\boldsymbol{\xi})$ ;
  end
end

```

Algorithm 2: Implementation with dimension reduction.

subproblem interface. We expect the exchanged information to have such a low effective stochastic dimension in multi-physics problems when that information consists of a solution field that has been smoothed by a forward operator, and in multi-scale problems when it is obtained by summarizing a fine-scale quantity into a coarse-scale representation.

3. Dimension reduction via Karhunen-Loeve decomposition

We will now recall the KL decomposition of classical stochastic processes, and then describe an adaptation of the KL decomposition to allow for the reduced representation of random variables with values in Hilbert spaces.

3.1. Motivation

In the research area of stochastic modeling and analysis, the KL decomposition is best known as a tool to reduce stochastic processes that describe uncertain *fields of coefficients and/or boundary conditions* of stochastic partial differential equations. This application of the KL decomposition makes use of the classical description of stochastic processes as indexed collections of random variables. In this work, however, the KL decomposition is rather used to reduce the *solution* of stochastic models, or to reduce quantities of interest that depend on that solution through a specified mapping. The solution of many stochastic models, including the solution of many stochastic partial differential equations, is not always amenable to a description as a classical stochastic process, and is often better described as a random variable that takes its values in a function space. On the differences between the classical description of stochastic processes and their description as random variables with values in function spaces, see [21, 22] and the references therein. This distinction has repercussions on the manner in which second-order moments are defined, and function-analytic membership is exploited to construct a KL decomposition, as described next.

3.2. Case of classical stochastic processes

Let $\{q(\mathbf{x}, \cdot), \mathbf{x} \in \mathcal{D}\}$ be a stochastic process defined on a probability space $(\mathbb{R}^N, \mathcal{B}(\mathbb{R}^N), P_{\xi})$, indexed by a closed bounded subset \mathcal{D} of \mathbb{R}^d (with $d=1, 2$, or 3), and with values in \mathbb{R} . Let this stochastic process be of the second order, in that:

$$\int_{\mathbb{R}^N} |q(\mathbf{x}, \xi)|^2 dP_{\xi} < +\infty, \quad \forall \mathbf{x} \in \mathcal{D}. \quad (5)$$

We emphasize that the present case concerns the classical description of the stochastic process as an indexed collection of random variables: the value $q(\mathbf{x}, \cdot)$ taken by the stochastic process at each index \mathbf{x} in \mathcal{D} is a random variable defined on $(\mathbb{R}^N, \mathcal{B}(\mathbb{R}^N), P_{\xi})$ with values in \mathbb{R} .

3.2.1. Second-order descriptors As is well known, the first and second-order descriptors are meaningfully defined as follows. The mean is defined as a function \bar{q} from \mathcal{D} into \mathbb{R} such that:

$$\bar{q}(\mathbf{x}) = \int_{\mathbb{R}^N} q(\mathbf{x}, \xi) dP_{\xi}, \quad \forall \mathbf{x} \in \mathcal{D}, \quad (6)$$

and the covariance is a function C_q from $\mathcal{D} \times \mathcal{D}$ into \mathbb{R} such that:

$$C_q(\mathbf{x}, \mathbf{y}) = \int_{\mathbb{R}^N} \left(q(\mathbf{x}, \boldsymbol{\xi}) - \bar{q}(\mathbf{x}) \right) \left(q(\mathbf{y}, \boldsymbol{\xi}) - \bar{q}(\mathbf{y}) \right) dP_{\boldsymbol{\xi}}, \quad \forall \mathbf{x}, \mathbf{y} \in \mathcal{D}. \quad (7)$$

We note that these definitions of the second-order moments are consistent with the classical description of stochastic processes as indexed collections of random variables: the mean function associates to each index \mathbf{x} the mean of the random variable $q(\mathbf{x}, \cdot)$ at that index, and the covariance function associates to each pair of indices \mathbf{x} and \mathbf{y} the covariance of the random variables $q(\mathbf{x}, \cdot)$ and $q(\mathbf{y}, \cdot)$. Clearly, the covariance function is symmetric, in that:

$$C_q(\mathbf{x}, \mathbf{y}) = C_q(\mathbf{y}, \mathbf{x}), \quad \forall \mathbf{x}, \mathbf{y} \in \mathcal{D}. \quad (8)$$

Moreover, it is [21] of positive type, in that:

$$\sum_{i=1}^k \sum_{j=1}^k a_i a_j C_q(\mathbf{x}_i, \mathbf{x}_j) \geq 0, \quad \forall \{\mathbf{x}_1, \dots, \mathbf{x}_k\} \subset \mathcal{D}, \quad \forall \{a_1, \dots, a_k\} \subset \mathbb{R}, \quad \forall k \in \mathbb{N}. \quad (9)$$

Let the fluctuating part of the stochastic process be mean-square continuous, in that:

$$\lim_{\mathbf{y} \rightarrow \mathbf{x}} \int_{\mathbb{R}^N} \left| \left(q(\mathbf{x}, \boldsymbol{\xi}) - \bar{q}(\mathbf{x}) \right) - \left(q(\mathbf{y}, \boldsymbol{\xi}) - \bar{q}(\mathbf{y}) \right) \right|^2 dP_{\boldsymbol{\xi}} = 0, \quad \forall \mathbf{x} \in \mathcal{D}. \quad (10)$$

The covariance function is [21] then continuous. Since, in addition, \mathcal{D} was assumed to be closed and bounded, the covariance function is then square-integrable, in that:

$$\int_{\mathcal{D}} \int_{\mathcal{D}} |C_q(\mathbf{x}, \mathbf{y})|^2 d\mathbf{x} d\mathbf{y} < +\infty. \quad (11)$$

This property is exploited to use the covariance function as a kernel to define an integral operator \mathcal{C}_q from $L^2(\mathcal{D}, \mathbb{R})$ into $L^2(\mathcal{D}, \mathbb{R})$ such that:

$$\mathcal{C}_q(f) = \int_{\mathcal{D}} C_q(\mathbf{x}, \cdot) f(\mathbf{x}) d\mathbf{x}, \quad \forall f \in L^2(\mathcal{D}, \mathbb{R}), \quad (12)$$

where $L^2(\mathcal{D}, \mathbb{R})$ is the space of functions from \mathcal{D} into \mathbb{R} which are square-integrable, in that:

$$\int_{\mathcal{D}} |f(\mathbf{x})|^2 d\mathbf{x} < +\infty. \quad (13)$$

The square-integrability of the covariance function C_q implies [23] that the covariance operator \mathcal{C}_q is Hilbert-Schmidt. Moreover, since the covariance function is symmetric, the covariance operator is [24] self-adjoint, in that:

$$\mathcal{C}_q = \mathcal{C}_q^t, \quad (14)$$

in which the operator \mathcal{C}_q^t from $L^2(\mathcal{D}, \mathbb{R})$ into $L^2(\mathcal{D}, \mathbb{R})$ is the adjoint operator of \mathcal{C}_q , such that:

$$\int_{\mathcal{D}} (\mathcal{C}_q(f))(\mathbf{x}) g(\mathbf{x}) d\mathbf{x} = \int_{\mathcal{D}} f(\mathbf{x}) (\mathcal{C}_q^t(g))(\mathbf{x}) d\mathbf{x}, \quad \forall f, g \in L^2(\mathcal{D}, \mathbb{R}). \quad (15)$$

Finally, since the covariance function is of positive type, the covariance operator is [21, 24] positive, in that:

$$\int_{\mathcal{D}} (\mathcal{C}_q(f))(\mathbf{x}) f(\mathbf{x}) d\mathbf{x} \geq 0, \quad \forall f \in L^2(\mathcal{D}, \mathbb{R}). \quad (16)$$

3.2.2. KL decomposition Since the covariance operator \mathcal{C}_q is Hilbert-Schmidt and therefore compact, self-adjoint and positive, the solution to the eigenproblem:

$$\mathcal{C}_q(\varphi_i) = \lambda_i \varphi_i, \quad (17)$$

provides [23] a denumerable set of eigenfunctions $\{\varphi_i\}_{i=1}^{\infty}$, which constitutes a complete orthonormal basis of $L^2(\mathcal{D}, \mathbb{R})$, whereby all eigenvalues $\{\lambda_i\}_{i=1}^{\infty}$ are positive, square-summable in that $\sum_{i=1}^{\infty} \lambda_i^2 < +\infty$, and therefore λ_i tends to 0 as index i increases to infinity. The KL decomposition of $\{q(\mathbf{x}, \cdot), \mathbf{x} \in \mathcal{D}\}$ is [25, 26] then given by:

$$q(\mathbf{x}, \boldsymbol{\xi}) = \bar{q}(\mathbf{x}) + \sum_{i=1}^{\infty} \sqrt{\lambda_i} \varphi_i(\mathbf{x}) \eta_i(\boldsymbol{\xi}), \quad (18)$$

in which the η_i are random variables on $(\mathbb{R}^N, \mathcal{B}(\mathbb{R}^N), P_{\boldsymbol{\xi}})$ with values in \mathbb{R} , such that:

$$\eta_i(\boldsymbol{\xi}) = \frac{1}{\sqrt{\lambda_i}} \int_{\mathcal{D}} (q(\mathbf{x}, \boldsymbol{\xi}) - \bar{q}(\mathbf{x})) \varphi_i(\mathbf{x}) d\mathbf{x}, \quad (19)$$

Since the covariance function is continuous, the eigenfunctions are continuous, such that the integral (19) can be meaningfully defined as a mean-square Riemann integral. The expansion converges uniformly in mean-square, in that:

$$\lim_{n \rightarrow \infty} \int_{\mathbb{R}^N} \left| q(\mathbf{x}, \boldsymbol{\xi}) - \left(\bar{q}(\mathbf{x}) + \sum_{i=1}^n \sqrt{\lambda_i} \varphi_i(\mathbf{x}) \eta_i(\boldsymbol{\xi}) \right) \right|^2 dP_{\boldsymbol{\xi}} = 0, \quad \forall \mathbf{x} \in \mathcal{D}. \quad (20)$$

The coordinate functions φ_i are orthonormal in their inner product, in that:

$$\int_{\mathcal{D}} \varphi_i(\mathbf{x}) \varphi_j(\mathbf{x}) d\mathbf{x} = \delta_{ij}, \quad (21)$$

and the random variables η_i are zero-mean and orthonormal in their inner product:

$$\int_{\mathbb{R}^N} \eta_i(\boldsymbol{\xi}) dP_{\boldsymbol{\xi}} = 0, \quad (22)$$

$$\int_{\mathbb{R}^N} \eta_i(\boldsymbol{\xi}) \eta_j(\boldsymbol{\xi}) dP_{\boldsymbol{\xi}} = \delta_{ij}, \quad (23)$$

in which δ_{ij} is the Dirac delta, equal to 1 if $i = j$, and 0 otherwise.

3.3. Case of random variables that take their values in a Hilbert space

Let \mathbf{q} be a random variable defined on a probability space $(\mathbb{R}^N, \mathcal{B}(\mathbb{R}^N), P_{\boldsymbol{\xi}})$ which takes its values in a separable Hilbert space Q . Let $\langle \cdot, \cdot \rangle_Q$ denote the inner product on Q , and $\|\cdot\|_Q = \sqrt{\langle \cdot, \cdot \rangle_Q}$ the norm. Let the random variable \mathbf{q} be of the second order, in that:

$$\int_{\mathbb{R}^N} \|\mathbf{q}(\boldsymbol{\xi})\|_Q^2 dP_{\boldsymbol{\xi}} < +\infty. \quad (24)$$

This level of abstraction is very general: apart from the standard Euclidean spaces of vectors and matrices, examples of the Hilbert space Q include spaces of square-integrable functions, spaces of sequences, as well as Sobolev spaces, amongst many other possibilities.

3.3.1. Second-order descriptors The manner in which second-order descriptors and their properties are defined for random variables that take their values in a Hilbert space is different from the manner in which they are defined for classical stochastic processes. All definitions to follow are consistent with those that can be found in references [21, 22, 27, 28]. This time, the mean is defined as the linear function $m_{\mathbf{q}}$ from Q into \mathbb{R} such that:

$$m_{\mathbf{q}}(\mathbf{p}) = \int_{\mathbb{R}^N} \langle \mathbf{q}(\boldsymbol{\xi}), \mathbf{p} \rangle_Q dP_{\boldsymbol{\xi}}, \quad \forall \mathbf{p} \in Q \quad (25)$$

and the covariance is defined as the bilinear function $C_{\mathbf{q}}$ from $Q \times Q$ into \mathbb{R} such that:

$$C_{\mathbf{q}}(\mathbf{p}, \mathbf{r}) = \int_{\mathbb{R}^N} \left(\langle \mathbf{q}(\boldsymbol{\xi}), \mathbf{p} \rangle_Q - m_{\mathbf{q}}(\mathbf{p}) \right) \left(\langle \mathbf{q}(\boldsymbol{\xi}), \mathbf{r} \rangle_Q - m_{\mathbf{q}}(\mathbf{r}) \right) dP_{\boldsymbol{\xi}}, \quad \forall \mathbf{p}, \mathbf{r} \in Q \quad (26)$$

We note that these definitions are consistent with the function-analytic membership of the random variable \mathbf{q} , in that the membership of the realizations of \mathbf{q} to the Hilbert space Q implies that \mathbf{q} is analyzed most naturally through its projection onto fixed elements or basis vectors of Q . Indeed, the mean function associates to any fixed element \mathbf{p} of Q the mean of the random variable $\langle \mathbf{q}, \mathbf{p} \rangle_Q$ obtained by projecting \mathbf{q} onto \mathbf{p} , and the covariance function associates to any fixed pair of elements \mathbf{p} and \mathbf{r} of Q the covariance of the random variables $\langle \mathbf{q}, \mathbf{p} \rangle_Q$ and $\langle \mathbf{q}, \mathbf{r} \rangle_Q$. Clearly, the covariance function is symmetric, in that:

$$C_{\mathbf{q}}(\mathbf{p}, \mathbf{r}) = C_{\mathbf{q}}(\mathbf{r}, \mathbf{p}), \quad \forall \mathbf{p}, \mathbf{r} \in Q, \quad (27)$$

and positive, in that:

$$C_{\mathbf{q}}(\mathbf{p}, \mathbf{p}) \geq 0, \quad \forall \mathbf{p} \in Q. \quad (28)$$

It follows from (24) and Hölder's inequality that the mean function is continuous. Thus, there exists by the Riesz representation theorem a unique vector $\bar{\mathbf{q}}$ in Q , the mean vector, such that:

$$\langle \bar{\mathbf{q}}, \mathbf{p} \rangle_Q = m_{\mathbf{q}}(\mathbf{p}), \quad \forall \mathbf{p} \in Q. \quad (29)$$

Likewise, it follows from (24) and Hölder's inequality that the covariance function is continuous, and therefore by the Riesz representation theorem that there exists [23] a unique linear continuous operator $\mathcal{C}_{\mathbf{q}}$ from Q into Q , called the covariance operator, such that:

$$\langle \mathcal{C}_{\mathbf{q}}(\mathbf{p}), \mathbf{r} \rangle_Q = C_{\mathbf{q}}(\mathbf{p}, \mathbf{r}), \quad \forall \mathbf{p}, \mathbf{r} \in Q. \quad (30)$$

Let $\{\mathbf{e}_i\}_{i=1}^{\infty}$ be any complete orthonormal basis of Q ; since the Hilbert-Schmidt norm:

$$\sqrt{\sum_{i,j=1}^{\infty} \left(\langle \mathcal{C}_{\mathbf{q}}(\mathbf{e}_i), \mathbf{e}_j \rangle_Q \right)^2} = \sqrt{\sum_{i,j=1}^{\infty} \left(\int_{\mathbb{R}^N} \langle \mathbf{q}(\boldsymbol{\xi}) - \bar{\mathbf{q}}, \mathbf{e}_i \rangle_Q \langle \mathbf{q}(\boldsymbol{\xi}) - \bar{\mathbf{q}}, \mathbf{e}_j \rangle_Q dP_{\boldsymbol{\xi}} \right)^2} \quad (31)$$

$$\leq \sum_{i=1}^{\infty} \int_{\mathbb{R}^N} \langle \mathbf{q}(\boldsymbol{\xi}) - \bar{\mathbf{q}}, \mathbf{e}_i \rangle_Q^2 dP_{\boldsymbol{\xi}} \quad (32)$$

$$= \int_{\mathbb{R}^N} \|\mathbf{q}(\boldsymbol{\xi})\|_Q^2 dP_{\boldsymbol{\xi}} - \|\bar{\mathbf{q}}\|_Q^2, \quad (33)$$

is bounded due to (24), the covariance operator is [23] Hilbert-Schmidt. Moreover, since the covariance function is symmetric, the covariance operator is [21] self-adjoint, in that:

$$\mathcal{C}_{\mathbf{q}} = \mathcal{C}_{\mathbf{q}}^t, \quad (34)$$

in which the operator \mathcal{C}_q^t from Q into Q is the adjoint operator of \mathcal{C}_q , such that:

$$\langle \mathcal{C}_q(\mathbf{p}), \mathbf{r} \rangle_Q = \langle \mathbf{p}, \mathcal{C}_q^t(\mathbf{r}) \rangle_Q, \quad \forall \mathbf{p}, \mathbf{r} \in Q, \quad (35)$$

and, since the covariance function is positive, the covariance operator is positive, in that:

$$\langle \mathcal{C}_q(\mathbf{p}), \mathbf{p} \rangle_Q \geq 0, \quad \forall \mathbf{p} \in Q. \quad (36)$$

3.3.2. KL decomposition Since the covariance operator \mathcal{C}_q is Hilbert-Schmidt and therefore compact, self-adjoint and positive, the solution to the eigenproblem:

$$\mathcal{C}_q(\varphi_i) = \lambda_i \varphi_i, \quad (37)$$

provides a denumerable set of eigenvectors $\{\varphi_i\}_{i=1}^{\infty}$, which constitutes a complete orthonormal basis of Q , whereby all eigenvalues $\{\lambda_i\}_{i=1}^{\infty}$ are positive, square-summable in that $\sum_{i=1}^{\infty} \lambda_i^2 < +\infty$, and therefore λ_i tends to 0 as i goes to infinity. The KL decomposition then reads as:

$$\mathbf{q}(\boldsymbol{\xi}) = \bar{\mathbf{q}} + \sum_{i=1}^{\infty} \sqrt{\lambda_i} \varphi_i \eta_i(\boldsymbol{\xi}), \quad (38)$$

in which the η_i are random variables on $(\mathbb{R}^N, \mathcal{B}(\mathbb{R}^N), P_{\boldsymbol{\xi}})$ with values in \mathbb{R} , such that:

$$\eta_i(\boldsymbol{\xi}) = \frac{1}{\sqrt{\lambda_i}} \langle \mathbf{q}(\boldsymbol{\xi}) - \bar{\mathbf{q}}, \varphi_i \rangle_Q. \quad (39)$$

By the Hilbert-space orthogonal decomposition theorem, the decomposition converges strongly:

$$\lim_{n \rightarrow \infty} \int_{\mathbb{R}^N} \left\| \mathbf{q}(\boldsymbol{\xi}) - \left(\bar{\mathbf{q}} + \sum_{i=1}^n \sqrt{\lambda_i} \varphi_i \eta_i(\boldsymbol{\xi}) \right) \right\|_Q^2 dP_{\boldsymbol{\xi}} = 0. \quad (40)$$

The coordinate functions φ_i are orthonormal in their inner product, in that:

$$\langle \varphi_i, \varphi_j \rangle_Q = \delta_{ij}, \quad (41)$$

and the random variables η_i are zero-mean and orthonormal in their inner product:

$$\int_{\mathbb{R}^N} \eta_i(\boldsymbol{\xi}) dP_{\boldsymbol{\xi}} = 0, \quad (42)$$

$$\int_{\mathbb{R}^N} \eta_i(\boldsymbol{\xi}) \eta_j(\boldsymbol{\xi}) dP_{\boldsymbol{\xi}} = \delta_{ij}. \quad (43)$$

The truncation of the KL decomposition after n terms yields a partial sum:

$$\mathbf{q}^n(\boldsymbol{\eta}(\boldsymbol{\xi})) = \bar{\mathbf{q}} + \sum_{i=1}^n \sqrt{\lambda_i} \varphi_i \eta_i(\boldsymbol{\xi}), \quad (44)$$

which provides an approximation \mathbf{q}^n of the random variable \mathbf{q} . This approximation is optimal [7], in that, of all linear expansions containing n orthonormal basis vectors $\mathbf{e}_1, \dots, \mathbf{e}_n$ in Q , it minimizes the mean-square norm of the approximation error:

$$\int_{\mathbb{R}^N} \left\| \mathbf{q}(\boldsymbol{\xi}) - \mathbf{q}^n(\boldsymbol{\eta}(\boldsymbol{\xi})) \right\|_Q^2 dP_{\boldsymbol{\xi}} = \min_{\substack{\{\mathbf{e}_1, \dots, \mathbf{e}_n\} \subset Q \\ \langle \mathbf{e}_i, \mathbf{e}_j \rangle_Q = \delta_{ij}}} \int_{\mathbb{R}^N} \left\| \mathbf{q}(\boldsymbol{\xi}) - \left(\bar{\mathbf{q}} + \sum_{i=1}^n \mathbf{e}_i \langle \mathbf{q}(\boldsymbol{\xi}) - \bar{\mathbf{q}}, \mathbf{e}_i \rangle_Q \right) \right\|_Q^2 dP_{\boldsymbol{\xi}}. \quad (45)$$

4. Implementation

4.1. Discretization using stochastic expansion methods

Without loss of generality, we assume $P_{\boldsymbol{\xi}} = P_{\xi_1} \times \dots \times P_{\xi_N}$ is a product distribution, that is to say that the uncertain parameters ξ_1, \dots, ξ_N are statistically independent (for a set of dependent parameters, an appropriate technique, such as the Rosenblatt transformation, could be used to obtain a statistically equivalent set of independent parameters).

For each dimension $i = 1, \dots, N$, let H_i^0, \dots, H_i^P be the P_{ξ_i} -orthogonal polynomials up to degree P . These can be obtained by Gram-Schmidt orthonormalization of the monomials $1, \xi_i, \dots, \xi_i^P$, or read from tables in the literature if P_{ξ_i} is a "labeled" distribution.

Let $\{H_{\boldsymbol{\alpha}}, 0 \leq |\boldsymbol{\alpha}| \leq P\}$ denote the collection of tensor-product polynomials up to total degree P , in which $\boldsymbol{\alpha} = (\alpha_1, \dots, \alpha_N)$ is a multi-index in \mathbb{N}^N with $|\boldsymbol{\alpha}| = \alpha_1 + \dots + \alpha_N$, and $H_{\boldsymbol{\alpha}}(\boldsymbol{\xi}) = H_1^{\alpha_1}(\xi_1) \times \dots \times H_N^{\alpha_N}(\xi_N)$. The use of a stochastic expansion method for the solution of (3)-(4) then involves the representation of the solution by a PC expansion:

$$\mathbf{u}_1^P(\boldsymbol{\xi}) = \sum_{|\boldsymbol{\alpha}|=0}^P \mathbf{u}_{1\boldsymbol{\alpha}} H_{\boldsymbol{\alpha}}(\boldsymbol{\xi}), \quad \mathbf{u}_{1\boldsymbol{\alpha}} \in U_1, \quad (46)$$

$$\mathbf{u}_2^P(\boldsymbol{\xi}) = \sum_{|\boldsymbol{\alpha}|=0}^P \mathbf{u}_{2\boldsymbol{\alpha}} H_{\boldsymbol{\alpha}}(\boldsymbol{\xi}), \quad \mathbf{u}_{2\boldsymbol{\alpha}} \in U_2. \quad (47)$$

The task of the solution algorithm then lies in computing the coordinates $\mathbf{u}_{1\boldsymbol{\alpha}}$ and $\mathbf{u}_{2\boldsymbol{\alpha}}$ of the solution with respect to the polynomial chaos basis.

4.2. KL decomposition

We will now provide details concerning the implementation of the KL decomposition of random variables which take their values in a Hilbert space, which was outlined in Sec. 3.3. Specifically, we will consider the particular case of computing the KL decomposition of a second-order random variable \mathbf{q}^P defined on $(\mathbb{R}^N, \mathcal{B}(\mathbb{R}^N), P_{\boldsymbol{\xi}})$, which takes its values in a Hilbert space Q , and which is represented by a PC expansion of total degree P as:

$$\mathbf{q}^P(\boldsymbol{\xi}) = \sum_{|\boldsymbol{\alpha}|=0}^P \mathbf{q}_{\boldsymbol{\alpha}} H_{\boldsymbol{\alpha}}(\boldsymbol{\xi}), \quad \mathbf{q}_{\boldsymbol{\alpha}} \in Q. \quad (48)$$

Clearly, this particular case is the one needed in implementations of algorithms of the form of Algorithm 2. With reference to (25) and (29), the mean of \mathbf{q}^P is the vector $\bar{\mathbf{q}}$ in Q , such that:

$$\bar{\mathbf{q}} = \mathbf{q}_0. \quad (49)$$

Indeed, since the polynomial chaos satisfy $\int_{\mathbb{R}^N} H_{\boldsymbol{\alpha}}(\boldsymbol{\xi}) dP_{\boldsymbol{\xi}} = \delta_{\boldsymbol{\alpha}\mathbf{0}}$, we have:

$$\langle \bar{\mathbf{q}}, \mathbf{p} \rangle_Q = \langle \mathbf{q}_0, \mathbf{p} \rangle_Q = \int_{\mathbb{R}^N} \left\langle \sum_{|\boldsymbol{\alpha}|=0}^P \mathbf{q}_{\boldsymbol{\alpha}} H_{\boldsymbol{\alpha}}(\boldsymbol{\xi}), \mathbf{p} \right\rangle_Q dP_{\boldsymbol{\xi}} = \int_{\mathbb{R}^N} \langle \mathbf{q}^P(\boldsymbol{\xi}), \mathbf{p} \rangle_Q dP_{\boldsymbol{\xi}}, \quad \forall \mathbf{p} \in Q. \quad (50)$$

Let $\cdot \otimes \cdot$ denote the tensor product on Q , which maps any pair of vectors \mathbf{p}_1 and \mathbf{p}_2 in Q onto an operator $\mathbf{p}_1 \otimes \mathbf{p}_2$ from Q into Q such that $\langle (\mathbf{p}_1 \otimes \mathbf{p}_2)(\mathbf{r}_1), \mathbf{r}_2 \rangle_Q = \langle \mathbf{p}_1, \mathbf{r}_1 \rangle_Q \langle \mathbf{p}_2, \mathbf{r}_2 \rangle_Q$ for

all \mathbf{r}_1 and \mathbf{r}_2 in Q . With reference to (26) and (30), the covariance associated with \mathbf{q}^P is then the operator \mathcal{C}_q from Q into Q , such that:

$$\mathcal{C}_q = \sum_{|\alpha|=1}^P \mathbf{q}_\alpha \otimes \mathbf{q}_\alpha. \quad (51)$$

Indeed, since the polynomial chaos satisfy $\int_{\mathbb{R}^N} H_\alpha(\boldsymbol{\xi})H_\beta(\boldsymbol{\xi})dP_\xi = \delta_{\alpha\beta}$, we have:

$$\begin{aligned} \langle \mathcal{C}_q(\mathbf{p}), \mathbf{r} \rangle_Q &= \left\langle \left(\sum_{|\alpha|=1}^P \mathbf{q}_\alpha \otimes \mathbf{q}_\alpha \right) (\mathbf{p}), \mathbf{r} \right\rangle_Q \\ &= \int_{\mathbb{R}^N} \left\langle \sum_{|\alpha|=1}^P \mathbf{q}_\alpha H_\alpha(\boldsymbol{\xi}), \mathbf{p} \right\rangle_Q \left\langle \sum_{|\alpha|=1}^P \mathbf{q}_\alpha H_\alpha(\boldsymbol{\xi}), \mathbf{r} \right\rangle_Q dP_\xi \\ &= \int_{\mathbb{R}^N} \langle \mathbf{q}^P(\boldsymbol{\xi}) - \bar{\mathbf{q}}, \mathbf{p} \rangle_Q \langle \mathbf{q}^P(\boldsymbol{\xi}) - \bar{\mathbf{q}}, \mathbf{r} \rangle_Q dP_\xi, \end{aligned} \quad (52)$$

for any \mathbf{p} and \mathbf{r} in Q . With reference to (37), the construction of the KL decomposition requires the solution of the eigenproblem $\mathcal{C}_q(\boldsymbol{\varphi}_i) = \lambda_i \boldsymbol{\varphi}_i$. This eigenproblem is discretized by Galerkin projection onto a finite-dimensional basis. Specifically, given a collection $\{\boldsymbol{\psi}_k, 1 \leq k \leq \mu\}$ of (not necessarily orthogonal) basis vectors in Q , the eigenvectors are approximated as:

$$\boldsymbol{\varphi}_i^\mu = \sum_{k=1}^{\mu} \varphi_{ik} \boldsymbol{\psi}_k, \quad \varphi_{ik} \in \mathbb{R}, \quad (53)$$

and the coordinates φ_{ik} are computed by solving the generalized eigenproblem:

$$\begin{aligned} &\begin{bmatrix} \sum_{|\alpha|=1}^P \langle \mathbf{q}_\alpha, \boldsymbol{\psi}_1 \rangle_Q \langle \mathbf{q}_\alpha, \boldsymbol{\psi}_1 \rangle_Q & \cdots & \sum_{|\alpha|=1}^P \langle \mathbf{q}_\alpha, \boldsymbol{\psi}_1 \rangle_Q \langle \mathbf{q}_\alpha, \boldsymbol{\psi}_\mu \rangle_Q \\ \vdots & & \vdots \\ \sum_{|\alpha|=1}^P \langle \mathbf{q}_\alpha, \boldsymbol{\psi}_\mu \rangle_Q \langle \mathbf{q}_\alpha, \boldsymbol{\psi}_1 \rangle_Q & \cdots & \sum_{|\alpha|=1}^P \langle \mathbf{q}_\alpha, \boldsymbol{\psi}_\mu \rangle_Q \langle \mathbf{q}_\alpha, \boldsymbol{\psi}_\mu \rangle_Q \end{bmatrix} \begin{bmatrix} \varphi_{i1} \\ \vdots \\ \varphi_{i\mu} \end{bmatrix} \\ &= \lambda_i \begin{bmatrix} \langle \boldsymbol{\psi}_1, \boldsymbol{\psi}_1 \rangle_Q & \cdots & \langle \boldsymbol{\psi}_1, \boldsymbol{\psi}_\mu \rangle_Q \\ \vdots & & \vdots \\ \langle \boldsymbol{\psi}_\mu, \boldsymbol{\psi}_1 \rangle_Q & \cdots & \langle \boldsymbol{\psi}_\mu, \boldsymbol{\psi}_\mu \rangle_Q \end{bmatrix} \begin{bmatrix} \varphi_{i1} \\ \vdots \\ \varphi_{i\mu} \end{bmatrix}. \end{aligned} \quad (54)$$

Once (54) is solved, the KL decomposition is obtained as:

$$\mathbf{q}^\mu(\boldsymbol{\eta}^P(\boldsymbol{\xi})) = \bar{\mathbf{q}} + \sum_{i=1}^{\mu} \sqrt{\lambda_i} \boldsymbol{\varphi}_i^\mu \eta_i^P(\boldsymbol{\xi}), \quad (55)$$

with:

$$\eta_i^P(\boldsymbol{\xi}) = \frac{1}{\sqrt{\lambda_i}} \langle \mathbf{q}^P(\boldsymbol{\xi}) - \bar{\mathbf{q}}, \boldsymbol{\varphi}_i^\mu \rangle_Q. \quad (56)$$

The eigenvectors $\boldsymbol{\varphi}_i^\mu$ are orthonormal in their inner product:

$$\langle \boldsymbol{\varphi}_i^\mu, \boldsymbol{\varphi}_j^\mu \rangle_Q = \delta_{ij}, \quad (57)$$

and the random variables η_i^P are zero mean and orthonormal in their inner product:

$$\int_{\mathbb{R}^N} \eta_i^P(\boldsymbol{\xi}) dP_{\boldsymbol{\xi}} = 0, \quad (58)$$

$$\int_{\mathbb{R}^N} \eta_i^P(\boldsymbol{\xi}) \eta_j^P(\boldsymbol{\xi}) dP_{\boldsymbol{\xi}} = \delta_{ij}. \quad (59)$$

Upon injecting (48) in (56), a representation of each random variable η_i^P as a PC expansion is obtained:

$$\eta_i^P(\boldsymbol{\xi}) = \sum_{|\boldsymbol{\alpha}|=1}^P \eta_{i\boldsymbol{\alpha}} H_{\boldsymbol{\alpha}}(\boldsymbol{\xi}) = \sum_{|\boldsymbol{\alpha}|=1}^P \frac{1}{\sqrt{\lambda_i}} \langle \mathbf{q}_{\boldsymbol{\alpha}}, \boldsymbol{\varphi}_i^{\mu} \rangle_Q H_{\boldsymbol{\alpha}}(\boldsymbol{\xi}). \quad (60)$$

The coordinates $\eta_{i\boldsymbol{\alpha}}$ thus obtained provide a complete probabilistic characterization of the reduced random variables η_i^P .

4.3. Putting things together

Algorithm 3 demonstrates an implementation of the framework, which adopts the non-intrusive stochastic projection method [8] for the discretization of the random dimension. This algorithm requires a quadrature rule for integration with respect to $P_{\boldsymbol{\xi}}$. Fully-tensorized or sparse-grid multi-dimensional quadrature rules [29] synthesized from Gaussian or other suitable one-dimensional quadrature rules suggest themselves, in addition to Monte Carlo integration.

It should be noted that other stochastic expansion methods, such as embedded projection or collocation can also be adopted to solve the subproblems to obtain representations of their solution as PC expansions. However, this is not explicitly shown here for the sake of brevity.

5. Realization for a stochastic multi-physics problem

We will now demonstrate the framework on an illustration problem relevant to nuclear reactors.

5.1. Problem setting

[Figure 1 about here.]

We consider the stationary transport of neutrons in a one-dimensional reactor with a temperature feedback [30]. Let the reactor occupy the open interval $]0, L[$ (Fig. 1). The problem then consists in finding the neutron flux Φ and temperature T such that:

$$\frac{d}{dx} \left(D(T) \frac{d\Phi}{dx} \right) - \left(\Sigma_a(T) - \nu \Sigma_f(T) \right) \Phi = -s, \quad (61)$$

$$\frac{d}{dx} \left(k \frac{dT}{dx} \right) - h(T - T_{\infty}) = -E_f \Sigma_f(T) \Phi, \quad (62)$$

with homogeneous Neumann boundary conditions. The first term on the left-hand side of (61) represents neutron diffusion, the second term describes the net effect of the absorption and generation of neutrons, and the right-hand side is a distributed neutron source. The first term of the left-hand side of (62) represents heat conduction, the second term describes transmission of

```

Input : initialization
          quadrature formula  $\{(\boldsymbol{\xi}_k, W_k), 1 \leq k \leq \nu_R\}$  for integration w.r.t.  $P_\xi$ ;
while (not converged) do
   $\ell = \ell + 1$ ;
  first subproblem
    for  $k = 1$  to  $\nu_R$  do
      | Solve  $\mathbf{f}_1(\star, \hat{\mathbf{q}}_2^{(\ell-1)}(\boldsymbol{\xi}_k), \boldsymbol{\xi}_k) = \mathbf{0}$  for  $\hat{\mathbf{u}}_1^{(\ell)}(\boldsymbol{\xi}_k)$ ;
    end
    Compute PC coordinates of  $\hat{\mathbf{u}}_1^{P(\ell)}$  and  $\hat{\mathbf{q}}_1^{P(\ell)}$  by non-intrusive projection:
      
$$\hat{\mathbf{u}}_{1\alpha}^{(\ell)} = \sum_{k=1}^{\nu_R} \hat{\mathbf{u}}_1^{(\ell)}(\boldsymbol{\xi}_k) H_\alpha(\boldsymbol{\xi}_k) W_k,$$

      
$$\hat{\mathbf{q}}_{1\alpha}^{(\ell)} = \sum_{k=1}^{\nu_R} \mathbf{g}_1(\hat{\mathbf{u}}_1^{(\ell)}(\boldsymbol{\xi}_k), \boldsymbol{\xi}_k) H_\alpha(\boldsymbol{\xi}_k) W_k.$$

    end
    hand-shaking region
      | Approximate  $\hat{\mathbf{q}}_1^{P(\ell)}(\boldsymbol{\xi})$  by KL  $\hat{\mathbf{q}}_1^{n(\ell)}(\boldsymbol{\eta}(\boldsymbol{\xi})) = \bar{\mathbf{q}}_1^{(\ell)} + \sum_{i=1}^n \sqrt{\lambda_i^{(\ell)}} \boldsymbol{\varphi}_i^{(\ell)} \eta_i^{(\ell)}(\boldsymbol{\xi})$ ;
    end
    second subproblem
      for  $k = 1$  to  $\nu_R$  do
        | Solve  $\mathbf{f}_2(\hat{\mathbf{q}}_1^{n(\ell)}(\boldsymbol{\xi}_k), \star) = \mathbf{0}$  for  $\hat{\mathbf{u}}_2^{(\ell)}(\boldsymbol{\xi}_k)$ ;
      end
      Compute PC coordinates of  $\hat{\mathbf{u}}_2^{P(\ell)}$  and  $\hat{\mathbf{q}}_2^{P(\ell)}$  by non-intrusive projection:
        
$$\hat{\mathbf{u}}_{2\alpha}^{(\ell)} = \sum_{k=1}^{\nu_R} \hat{\mathbf{u}}_2^{(\ell)}(\boldsymbol{\xi}_k) H_\alpha(\boldsymbol{\xi}_k) W_k,$$

        
$$\hat{\mathbf{q}}_{2\alpha}^{(\ell)} = \sum_{k=1}^{\nu_R} \mathbf{g}_2(\hat{\mathbf{u}}_2^{(\ell)}(\boldsymbol{\xi}_k)) H_\alpha(\boldsymbol{\xi}_k) W_k.$$

      end
    end
  end

```

Algorithm 3: Implementation with dimension reduction.

heat to surroundings, and the right-hand side is a distributed heat source, which is proportional to the product of the fission cross-section and the neutron flux.

The coefficients D , Σ_a and Σ_f are the neutron diffusion constant, fission cross-section, and absorption cross-section, and are assumed to depend on the temperature as follows:

$$D(T(x)) = \begin{cases} D_{\text{ref}} \sqrt{\frac{T_{\text{min}}}{T_{\text{ref}}}} & \text{if } T(x) \leq T_{\text{min}} \\ D_{\text{ref}} \sqrt{\frac{T(x)}{T_{\text{ref}}}} & \text{if } T_{\text{min}} \leq T(x) \leq T_{\text{max}} \\ D_{\text{ref}} \sqrt{\frac{T_{\text{max}}}{T_{\text{ref}}}} & \text{if } T(x) \geq T_{\text{max}} \end{cases}, \quad (63)$$

$$\Sigma_a(T(x)) = \begin{cases} \Sigma_{a,\text{ref}} \sqrt{\frac{T_{\text{ref}}}{T_{\text{min}}}} & \text{if } T(x) \leq T_{\text{min}} \\ \Sigma_{a,\text{ref}} \sqrt{\frac{T_{\text{ref}}}{T(x)}} & \text{if } T_{\text{min}} \leq T(x) \leq T_{\text{max}} \\ \Sigma_{a,\text{ref}} \sqrt{\frac{T_{\text{ref}}}{T_{\text{max}}}} & \text{if } T(x) \geq T_{\text{max}} \end{cases}, \quad (64)$$

$$\Sigma_f(T(x)) = \begin{cases} \Sigma_{f,\text{ref}} \sqrt{\frac{T_{\text{ref}}}{T_{\text{min}}}} & \text{if } T(x) \leq T_{\text{min}} \\ \Sigma_{f,\text{ref}} \sqrt{\frac{T_{\text{ref}}}{T(x)}} & \text{if } T_{\text{min}} \leq T(x) \leq T_{\text{max}} \\ \Sigma_{f,\text{ref}} \sqrt{\frac{T_{\text{ref}}}{T_{\text{max}}}} & \text{if } T(x) \geq T_{\text{max}} \end{cases}. \quad (65)$$

The coefficients k and h are the heat conductivity and transmittivity. Finally, ν and E_f are the number of neutrons and the energy released per fission reaction.

5.2. Deterministic weak formulation

Let $V = H^1(]0, L[)$ and $W = H^1(]0, L[)$ be the spaces of functions that are sufficiently regular to describe the solution of the neutron and heat problem. The weak formulation then consists in finding Φ in V and T in W such that:

$$\int_0^L D(T) \frac{d\Phi}{dx} \frac{d\Psi}{dx} dx + \int_0^L (\Sigma_a(T) - \nu \Sigma_f(T)) \Phi \Psi dx = \int_0^L s \Psi dx, \quad \forall \Psi \in V, \quad (66)$$

$$\int_0^L k \frac{dT}{dx} \frac{dS}{dx} dx + \int_0^L h(T - T_\infty) S dx = \int_0^L E_f \Sigma_f(T) \Phi S dx, \quad \forall S \in W. \quad (67)$$

5.3. Random thermal transmittivity

Uncertainties are accommodated by modeling the thermal transmittivity by a random field $\{h(x, \cdot), 1 \leq x \leq L\}$ such that:

$$h(x, \boldsymbol{\xi}) = \bar{h} \left(1 + \delta \sum_{i=1}^N \sqrt{\lambda_i} \varphi_i(x) \sqrt{3} \xi_i \right), \quad P_{\boldsymbol{\xi}} - \text{a.s.}, \quad (68)$$

in which the ξ_i are independent uniform random variables with values in $[-1, 1]$, and therefore the $\sqrt{3}\xi_i$ are independent uniform random variables with zero mean and unit standard deviation, and the λ_i and φ_i are the eigenvalues and eigenmodes of the eigenproblem $\mathcal{C}(\varphi_i) = \lambda_i \varphi_i$, in which \mathcal{C} is the integral operator whose kernel is the covariance function:

$$C(x, y) = \frac{4a^2}{\pi^2(x-y)^2} \sin^2 \left(\frac{\pi(x-y)}{2a} \right). \quad (69)$$

The parameter a is the spatial correlation length of $\{h(x, \cdot), 1 \leq x \leq L\}$. Clearly, the random field $\{h(x, \cdot), 1 \leq x \leq L\}$ thus obtained is such that, at every position x , the random variable $h(x, \cdot)$ has mean \bar{h} and coefficient of variation δ (apart from the approximation error incurred by truncating the expansion after N terms).

5.4. Stochastic weak formulation

The weak formulation of the stochastic problem consists in finding random variables Φ and T defined on $(\mathbb{R}^N, \mathcal{B}(\mathbb{R}^N), P_\xi)$ valued in V and W , such that:

$$\int_0^L D(T(\xi)) \frac{d\Phi}{dx}(\xi) \frac{d\Psi}{dx} dx + \int_0^L (\Sigma_a(T(\xi)) - \nu \Sigma_f(T(\xi))) \Phi(\xi) \Psi dx = \int_0^L s \Psi dx, \quad \forall \Psi \in V, P_\xi\text{-a.s.}, \quad (70)$$

$$\int_0^L k \frac{dT}{dx}(\xi) \frac{dS}{dx} dx + \int_0^L h(\xi) (T(\xi) - T_\infty) S dx = \int_0^L E_f \Sigma_f(T(\xi)) \Phi(\xi) S dx, \quad \forall S \in W, P_\xi\text{-a.s.} \quad (71)$$

5.5. Discretization of space

The Finite Element (FE) method is used for spatial discretization. The domain $[0, L]$ is meshed using $\mu - 1$ elements of equal length h . Let N_1, \dots, N_μ then be a basis of element-wise linear shape functions, such that N_k takes the value 1 at the k -th node, and 0 at the other nodes. These allow for the approximation of any neutron flux Ψ and temperature S by:

$$\Psi^h(x) = \sum_{k=1}^{\mu} \Psi_k N_k(x), \quad \Psi_k \in \mathbb{R}, \quad (72)$$

$$S^h(x) = \sum_{k=1}^{\mu} S_k N_k(x), \quad S_k \in \mathbb{R}. \quad (73)$$

The FE discretization of the stochastic weak formulation (70)-(71) then consists in finding random vectors Φ and T with values in \mathbb{R}^μ , which collect the nodal values of the random neutron flux and temperature, such that:

$$\left[D(T(\xi)) + M(T(\xi)) \right] \Phi(\xi) = s, \quad P_\xi - \text{a.s.}, \quad (74)$$

$$\left[K + H(\xi) \right] T(\xi) = q(\Phi(\xi), T(\xi)), \quad P_\xi - \text{a.s.}, \quad (75)$$

with $D(T)$, $M(T)$, K , H , s and $q(\Phi, T)$ μ -dimensional matrices and vectors, such that:

$$\langle D(T) \Psi_1, \Psi_2 \rangle = \int_0^L D(T^h) \frac{d\Psi_1^h}{dx} \frac{d\Psi_2^h}{dx} dx, \quad (76)$$

$$\langle M(T) \Psi_1, \Psi_2 \rangle = \int_0^L (\Sigma_a(T^h) - \nu \Sigma_f(T^h)) \Psi_1^h \Psi_2^h dx, \quad (77)$$

$$\langle K S_1, S_2 \rangle = \int_0^L k \frac{dS_1^h}{dx} \frac{dS_2^h}{dx} dx, \quad (78)$$

$$\langle H S_1, S_2 \rangle = \int_0^L h S_1^h S_2^h dx, \quad (79)$$

$$\langle s, \Psi \rangle = \int_0^L s \Psi^h dx, \quad (80)$$

$$\langle q(T, \Phi), S \rangle = \int_0^L E_f \Sigma_f(T^h) \Phi^h S^h dx + \int_0^L h T_\infty S^h dx. \quad (81)$$

5.6. KL decomposition of the temperature

Since it is the solution of the second-order elliptic PDE (71), the random variable T^h is described naturally as a random variable defined on $(\mathbb{R}^N, \mathcal{B}(\mathbb{R}^N), P_{\xi})$ with values in the Sobolev space $H^1(]0, L[)$ of square-integrable functions with square-integrable derivative on $]0, L[$. Let T^h be approximated by a PC expansion as:

$$T^{hP}(\xi) = \sum_{|\alpha|=0}^P T_{\alpha}^h H_{\alpha}(\xi), \quad T_{\alpha}^h \in H^1(]0, L[). \quad (82)$$

The mean and covariance of T^{hP} are then:

$$\bar{T}^h = T_0^h, \quad (83)$$

$$C_T = \sum_{|\alpha|=1}^P T_{\alpha}^h \otimes T_{\alpha}^h. \quad (84)$$

The eigenvalues λ_i and eigenvectors

$$\varphi_i^h(x) = \sum_{k=1}^{\mu} \varphi_{ik} N_k(x), \quad \varphi_{ik} \in \mathbb{R}, \quad (85)$$

of $C_T(\varphi_i^h) = \lambda_i \varphi_i^h$ are obtained numerically by solving the generalized eigenproblem:

$$\begin{aligned} & \begin{bmatrix} \sum_{|\alpha|=1}^P \langle T_{\alpha}^h, N_1 \rangle_{H^1} \langle T_{\alpha}^h, N_1 \rangle_{H^1} & \dots & \sum_{|\alpha|=1}^P \langle T_{\alpha}^h, N_1 \rangle_{H^1} \langle T_{\alpha}^h, N_{\mu} \rangle_{H^1} \\ \vdots & & \vdots \\ \sum_{|\alpha|=1}^P \langle T_{\alpha}^h, N_{\mu} \rangle_{H^1} \langle T_{\alpha}^h, N_1 \rangle_{H^1} & \dots & \sum_{|\alpha|=1}^P \langle T_{\alpha}^h, N_{\mu} \rangle_{H^1} \langle T_{\alpha}^h, N_{\mu} \rangle_{H^1} \end{bmatrix} \begin{bmatrix} \varphi_{i1} \\ \vdots \\ \varphi_{i\mu} \end{bmatrix} \\ &= \lambda_i \begin{bmatrix} \langle N_1, N_1 \rangle_{H^1} & \dots & \langle N_1, N_{\mu} \rangle_{H^1} \\ \vdots & & \vdots \\ \langle N_{\mu}, N_1 \rangle_{H^1} & \dots & \langle N_{\mu}, N_{\mu} \rangle_{H^1} \end{bmatrix} \begin{bmatrix} \varphi_{i1} \\ \vdots \\ \varphi_{i\mu} \end{bmatrix}, \end{aligned} \quad (86)$$

in which the inner product $\langle \cdot, \cdot \rangle_{H^1}$ is such that $\langle S_1, S_2 \rangle_{H^1} = \int_0^L S_1 S_2 dx + \int_0^L (dS_1/dx)(dS_2/dx)dx$ for any pair S_1 and S_2 of functions in $H^1(]0, L[)$. The random variable T^h is then approximated by a truncated KL decomposition as:

$$T^n(\eta^P(\xi)) = \bar{T}^h + \sum_{i=1}^n \sqrt{\lambda_i} \varphi_i^h \eta_i^P(\xi), \quad (87)$$

in which each η_i^P is obtained as a PC expansion with the following coordinates:

$$\eta_i^P(\xi) = \sum_{|\alpha|=1}^P \eta_{i,\alpha} H_{\alpha}(\xi) = \sum_{|\alpha|=1}^P \frac{1}{\sqrt{\lambda_i}} \langle T_{\alpha}^h, \varphi_i^h \rangle_{H^1} H_{\alpha}(\xi). \quad (88)$$

5.7. Putting things together

Algorithm 4 outlines an implementation, which adopts the non-intrusive stochastic projection method for the discretization of the random dimension.


```

Input : initialization
          quadrature formula  $\{(\boldsymbol{\xi}_k, W_k), 1 \leq k \leq \nu_R\}$  for integration w.r.t.  $P_{\boldsymbol{\xi}}$ ;
while (not converged) do
   $\ell = \ell + 1$ ;
  heat-transfer problem
  for  $k = 1$  to  $\nu_R$  do
    Solve  $[K + H(\boldsymbol{\xi}_k)] \hat{T}^{(\ell)}(\boldsymbol{\xi}_k) = \hat{q}^{P(\ell-1)}(\boldsymbol{\xi}_k)$ ;
  end
  Compute PC coordinates of  $\hat{T}^{P(\ell)}$  by non-intrusive projection:
  
$$\hat{T}_{\alpha}^{(\ell)} = \sum_{k=1}^{\nu_R} \hat{T}^{(\ell)}(\boldsymbol{\xi}_k) H_{\alpha}(\boldsymbol{\xi}_k) W_k;$$

end
  hand-shaking region
  Approximate  $\hat{T}^{P(\ell)}(\boldsymbol{\xi})$  by KL  $\hat{T}^{n(\ell)}(\boldsymbol{\eta}^{P(\ell)}(\boldsymbol{\xi})) = \bar{T}^{(\ell)} + \sum_{i=1}^n \sqrt{\lambda_i^{(\ell)}} \varphi_i^{(\ell)} \eta_i^{P(\ell)}(\boldsymbol{\xi})$ ;
end
  neutron-transport problem
  for  $k = 1$  to  $\nu_R$  do
    Solve  $[D(\hat{T}^{n(\ell)}(\boldsymbol{\eta}^{P(\ell)}(\boldsymbol{\xi}_k))) + M(\hat{T}^{n(\ell)}(\boldsymbol{\eta}^{P(\ell)}(\boldsymbol{\xi}_k)))] \hat{\Phi}^{(\ell)}(\boldsymbol{\xi}_k) = s$ ;
  end
  Compute PC coordinates of  $\hat{\Phi}^{P(\ell)}$  and  $\hat{q}^{P(\ell)}$  by non-intrusive projection:
  
$$\hat{\Phi}_{\alpha}^{(\ell)} = \sum_{k=1}^{\nu_r} \hat{\Phi}^{(\ell)}(\boldsymbol{\xi}_k) H_{\alpha}(\boldsymbol{\xi}_k) W_k;$$

  
$$\hat{q}_{\alpha}^{(\ell)} = \sum_{k=1}^{\nu_r} \hat{q}(\hat{T}^{n(\ell)}(\boldsymbol{\eta}^{P(\ell)}(\boldsymbol{\xi}_k)), \hat{\Phi}^{n(\ell)}(\boldsymbol{\xi}_k)) H_{\alpha}(\boldsymbol{\xi}_k) W_k;$$

end
end

```

Algorithm 4: Implementation of the illustration problem.

6. Numerical results

Numerical results are presented for a problem with the following properties. The reactor is assumed to have dimension $L = 100$ cm. Deterministic and position-independent values are assumed for the neutron-diffusion constant $D_{\text{ref}} = 2.2$ cm, absorption cross-section $\Sigma_{\text{a,ref}} = 0.0195$ cm $^{-1}$, fission cross-section $\Sigma_{\text{a,ref}} = 0.0075$ cm $^{-1}$, multiplication factor $\nu = 2.2$, neutron source $s = 5.0E11$ neutrons/s/cm 3 , ambient temperature $T_{\infty} = 390$ K, fission energy $E_f = 3.0E-11$ J/neutrons, and temperatures $T_{\text{ref}} = 390$ K, $T_{\text{min}} = 390$ K and $T_{\text{max}} = 1000$ K. The random thermal transmittivity field has position-independent mean value $\bar{h} = 0.17$ J/K/cm 3 /s, spatial correlation length $a = 15$ cm, and coefficient of variation $\delta = 10\%$.

[Figure 2 about here.]

The thermal transmittivity field is defined by retaining $N = 10$ terms in the expansion (68). Figure 2(a) shows a few sample paths of the random field $\{h(x, \cdot), 0 \leq x \leq L\}$ thus obtained. Figure 2(b) shows the 10 largest-magnitude eigenvalues of the integral operator that has the covariance function (69) as its kernel.

6.1. Monte Carlo sampling-based implementation

[Figure 3 about here.]

A Monte Carlo simulation has been carried out with the stochastic model. First, $MC = 25000$ independent samples paths of the thermal transmittivity random field have been generated. To each of these samples is associated a deterministic multi-physics model. Each of these deterministic multi-physics models has been solved using the FE method for the spatial discretization and Gauss-Seidel successive substitution. Converged results have systematically been obtained for $\mu - 1 = 40$ finite elements and 20 iterations of the nonlinear solver.

Figure 3 shows a few samples of the random neutron flux and temperature thus obtained for the thermal conductivity taken equal to $k = 1 \text{ J/K/cm/s}$, $k = 10 \text{ J/K/cm/s}$, and $k = 100 \text{ J/K/cm/s}$. The samples of the predicted random temperature (Fig. 3(b)) are observed to become smoother as the value of the thermal conductivity is increased, that is to say that they oscillate less rapidly as a function of the position as the significance of the diffusion of heat is increased. The diffusion of heat for large values of the thermal conductivity is observed to strongly dampen the non-uniformity of the temperature.

The random temperature is precisely the information that is communicated from the heat transfer problem (to which ξ_1, \dots, ξ_N are internal sources of uncertainty) to the neutron transport problem (to which ξ_1, \dots, ξ_N are exogenous sources of uncertainty). Fig. 3 suggests that the *effective stochastic dimension* of the random temperature decreases as the significance of the diffusion of heat increases, or, equivalently, as the magnitude of the thermal conductivity increases. All results to follow have been obtained with $k = 100 \text{ J/K/cm/s}$.

6.2. Elementary PC-based implementation

A solution algorithm of the form of Algorithm 1 has been implemented, which uses the non-intrusive stochastic projection method for the discretization of the random dimension, and Gauss-Seidel successive substitution as the nonlinear solver for the solution of the discretized problem. Numerical results have been obtained using up-to-order-5 PC expansions ($P = 1$ to 5), and using up-to-level-6 Smolyak sparse-grid Gauss-Legendre quadrature rules. Specifically, all results to follow have been obtained using $R = P+1$ as the level of the quadrature rule when computing the coordinates of a PC expansion of order P . While convergence as a function of P will be discussed later, we will now present detailed intermediate results for $P = 5$.

[Figure 4 about here.]

Figure 4 shows the convergence of the nonlinear solver as a function of the number of iterations. The Gauss-Seidel successive substitution process is observed to converge at an exponential rate until about iteration 10, when roundoff and linear-solver tolerances become dominant. All results to follow have been obtained using 20 iterations of the nonlinear solver.

[Figure 5 about here.]

[Figure 6 about here.]

Figure 5 shows the PC coordinates of the random neutron flux and temperature thus obtained. Figure 6 shows a few samples of the random neutron flux and temperature, which have been synthesized from these PC expansions. The samples shown in Fig. 6 for the elementary implementation have been synthesized on the basis of the same samples from P_{ξ} as those that had been used to generate the samples shown in Fig. 3(e,f) for the Monte Carlo simulation. The similarity of these samples suggests that the PC-based surrogate model not only provides a *global approximation* to the multi-physics model, but is also capable of accurately reproducing the *sample-wise* response.

[Figure 7 about here.]

The elementary PC-based simulation has been repeated for orders $P = 1$ to 5. Figure 7 shows that the distance between the solutions obtained through the Monte Carlo and elementary PC-based simulations decreases at an exponential rate as the order is increased.

6.3. PC-based implementation with dimension reduction

PC-based simulations with dimension reduction by Algo. 4 have been carried out. Results have been obtained using up-to-order-5 PC expansions ($P = 1$ to 5), and using dimension reductions retaining up to 5 terms ($n = 1$ to 5). While convergence as a function of P and n will be discussed later, we will now present detailed intermediate results for $P = 5$ and $n = 2$.

[Figure 8 about here.]

Figure 8 shows the convergence of the nonlinear solver as a function of the number of iterations. Similarly to Fig. 4, the Gauss-Seidel successive substitution process is observed to converge at an exponential rate until about iteration 10, when roundoff and linear-solver tolerances become dominant. All results to follow have been obtained using 20 iterations.

[Figure 9 about here.]

[Figure 10 about here.]

Algorithm 4 requires the computation of a KL decomposition of the random temperature at each iteration. Figure 9 shows the KL decomposition obtained at the last iteration. The eigenvalues (Fig. 9(b)) are observed to decay at a faster rate than those of the KL decomposition of the random thermal transmittivity field (Fig. 2(b)), which is consistent with our earlier observation that the temperature is smoothed by the effect of the heat diffusion term. The PC coordinates of η_1^P and η_2^P (Figs. 9(e,f)) provide a complete probabilistic characterization of the reduced random variables of the KL decomposition. Figure 10 shows the joint and marginal probability distributions of η_1^P and η_2^P . These have been obtained by generating $1E7$ independent samples from P_{ξ} , propagating these samples through the PC expansions, and applying a kernel density estimation technique. Figure 10 shows the probability distribution of η_1^P and η_2^P exhibits statistical dependence and is not uniform, nor has the form of any other "labeled" distribution.

[Figure 11 about here.]

[Figure 12 about here.]

Figure 11 shows the PC coordinates of the random neutron flux and temperature obtained as output of Algo. 4. Figure 12 shows a few samples of the random neutron flux and temperature synthesized from these PC expansions. The samples shown in Fig. 12 for the PC-based simulation with dimension reduction have been synthesized on the basis of the same samples from P_{ξ} as those that had been used to generate the samples shown in Fig. 3(e,f) for the Monte Carlo simulation. Similarly to Fig. 6, the similarity of these samples suggests that the PC-based surrogate model not only provides a *global approximation* to the multi-physics model, but is also capable of accurately reproducing the *sample-wise* response.

[Figure 13 about here.]

The PC-based simulation with dimension reduction has been repeated for the orders $P = 1$ to 5 of the PC expansions, and the numbers $n = 1$ to 5 of terms retained in the KL decomposition. Figure 13 shows that the distance between the solutions obtained through the Monte Carlo simulation and the PC-based simulation with dimension reduction can be decreased systematically by increasing the order of the PCEs and by retaining more terms in the KL decomposition. For polynomial orders P larger than 2, the approximation error incurred by the truncation of the KL decomposition of the random temperature is observed to dominate the approximation error incurred by the truncation of the PC expansions.

7. Conclusion

While many coupled models can be expected to be affected by a large number of sources of uncertainty, information that is communicated across physics or scale interfaces often resides in a much lower dimensional space. This argument naturally calls for the use of dimension-reduction techniques for the representation of exchanged information. This work has demonstrated the formulation and implementation of an adaptation of the KL decomposition to represent information as it is passed from model component to model component.

The range of validity of the proposed dimension reduction has been demonstrated on a stochastic multi-physics model of the transport of neutrons in a nuclear reactor with a temperature feedback. A parameter study has highlighted that the solution fields exchanged between the neutron-transport and heat-transfer equations have a low effective stochastic dimension when they are smoothed by the effect of significant diffusion processes. Numerical results have shown that the KL decomposition is then able to extract a low-dimensional representation of uncertainty as it crosses the physics interface, while maintaining accuracy in the solutions. Numerical convergence studies have shown that accuracy can be increased systematically by retaining more terms in the KL decomposition.

The low-dimensional interface created by the proposed dimension reduction approach can be exploited to enable a more computationally efficient, albeit still accurate, solution in a reduced-dimensional space. This can be achieved by performing key algorithmic operations, such as the construction of orthogonal polynomials and quadrature formulas, in terms of the reduced stochastic degrees of freedom of the reduced uncertainty representations that cross interfaces. This is the main computational benefit of the proposed dimension reduction approach, and we plan to explore solution algorithms of this form in forthcoming work [31, 32].

Acknowledgements

This work was supported by DOE through an ASCR grant.

references

- [1] S. Das, R. Ghanem, and J. Spall. Asymptotic sampling distribution for polynomial chaos representation from data: A maximum entropy and Fisher information approach. *SIAM Journal on Scientific Computing*, 5:2207–2234, 2008. DOI: 10.1137/060652105.
- [2] R. Ghanem and A. Doostan. On the construction and analysis of stochastic models: characterization and propagation of the errors associated with limited data. *Journal of Computational Physics*, 217:63–81, 2006. DOI: 10.1016/j.jcp.2006.01.037.
- [3] C. Soize. Maximum entropy approach for modeling random uncertainties in transient elastodynamics. *Journal of the Acoustical Society of America*, 109:1979–1996, 2001. DOI: 10.1121/1.1360716.
- [4] H. Cramér. *Mathematical Methods of Statistics*. Princeton University Press, 1946.
- [5] S. Kullback. *Information Theory and Statistics*. Dover Publications, 1968.
- [6] C. Robert and G. Casella. *Monte Carlo Statistical Methods*. Springer, 2005.
- [7] R. Ghanem and P. Spanos. *Stochastic Finite Elements: A Spectral Approach*. Dover, 2003.
- [8] C. Soize and R. Ghanem. Physical systems with random uncertainties: chaos representations with arbitrary probability measure. *SIAM Journal on Scientific Computing*, 26:395–410, 2004. DOI: 10.1137/S1064827503424505.
- [9] R. Ghanem. Hybrid stochastic finite elements and generalized Monte Carlo simulation. *Journal of Applied Mechanics*, 65:1004–1009, 1998. DOI: 10.1115/1.2791894.
- [10] R. Ghanem and D. Ghiocel. A new implementation of the spectral stochastic finite element method for stochastic constitutive relations. In *ASCE 12th Engineering Mechanics Conference*, La Jolla, California, USA, 1998.
- [11] D. Ghiocel and R. Ghanem. Stochastic finite-element analysis of seismic soilstructure interaction. *ASCE Journal of Engineering Mechanics*, 2002. DOI: 10.1061/(ASCE)0733-9399(2002)128:1(66).
- [12] D. Xiu and J. Hesthaven. High-order collocation methods for differential equations with random inputs. *SIAM Journal on Scientific Computing*, 27:1118–1139, 2005. DOI: 10.1137/040615201.
- [13] I. Babuska, F. Nobile, and R. Tempone. A stochastic collocation method for elliptic partial differential equations with random input data. *SIAM Journal on Numerical Analysis*, 45:1005–1034, 2007. DOI: 10.1137/050645142.

- [14] A. Doostan, R. Ghanem, and J. Red Horse. Stochastic model reduction for chaos representations. *Computer Methods in Applied Mechanics and Engineering*, 196:3951–3966, 2007. DOI: 10.1016/j.cma.2006.10.047.
- [15] K. Maute, G. Weickum, and M. Eldred. A reduced-order stochastic finite element approach for design optimization under uncertainty. *Structural Safety*, 31:450–459, 2009. DOI: 10.1016/j.strusafe.2009.06.004.
- [16] A. Nouy. A generalized spectral decomposition technique to solve a class of linear stochastic partial differential equations. *Computer Methods in Applied Mechanics and Engineering*, 196:4521–4537, 2007. DOI: 10.1016/j.cma.2007.05.016.
- [17] S. Boyaval, C. Le Bris, Y. Maday, N. Nguyen, and A. Patera. A reduced basis approach for variational problems with stochastic parameters: application to heat conduction with variable Robin coefficient. *Computer Methods in Applied Mechanics and Engineering*, 198:3187–3206, 2009. DOI: 10.1016/j.cma.2009.05.019.
- [18] S. Acharjee and N. Zabaras. A concurrent model reduction approach on spatial and random domains for the solution of stochastic PDEs. *International Journal for Numerical Methods in Engineering*, 66:1934–1954, 2006. DOI: 10.1002/nme.1611.
- [19] M. Guedri, N. Bouhaddi, and R. Majed. Reduction of the stochastic finite element models using a robust dynamic condensation method. *Journal of Sound and Vibration*, 297:123–145, 2006. DOI: 10.1016/j.jsv.2006.03.046.
- [20] S. Sachdeva, P. Nair, and A. Keane. Comparative study of projection schemes for stochastic finite element analysis. *Computer Methods in Applied Mechanics and Engineering*, 195:2371–2392, 2006. DOI: 10.1016/j.cma.2005.05.010.
- [21] P. Krée and C. Soize. *Mathematics of random phenomena*. Reidel Publishing Company, 1983.
- [22] J. Red Horse and R. Ghanem. Elements of a function analytic approach to probability. *International Journal for Numerical Methods in Engineering*, 80:689–716, 2009. DOI: 10.1002/nme.2643.
- [23] M. Reed and B. Simon. *Methods of mathematical physics*. Academic Press, 1980.
- [24] L. Schwartz. Sous-espaces hilbertiens d’espaces vectoriels topologiques et noyaux associés (noyaux reproduisants). *Journal d’Analyse Mathématique*, 13:115–256, 1964. DOI: 10.1007/BF02786620.
- [25] M. Loève. *Probability Theory II*. Springer, 1978.
- [26] A. Naylor and G. Sell. *Linear Operator Theory in Engineering and Science*. Springer, 2000.
- [27] N. Vakhania, V. Tarieladze, and S. Chobanyan. *Probability distributions on Banach spaces*. Reidel Publishing Company, 1987.
- [28] U. Grenander. *Probabilities on algebraic structures*. Dover, 2008.

- [29] M. Holtz. *Sparse Grid Quadrature in High Dimensions with Applications in Finance and Insurance*. Springer, 2010.
- [30] J. Lamarsh. *Introduction to Nuclear Reactor Theory*. American Nuclear Society, 2002.
- [31] M. Arnst, R. Ghanem, E. Phipps, and J. Red Horse. Measure transformation and efficient quadrature in reduced-dimensional stochastic analysis of coupled systems. *International Journal for Numerical Methods in Engineering*, 2011. In preparation.
- [32] M. Arnst, R. Ghanem, E. Phipps, and J. Red Horse. Uncertainty segregation and tensor-product-type approximation in reduced-dimensional stochastic analysis of coupled systems. *International Journal for Numerical Methods in Engineering*, 2011. In preparation.

List of Figures

1	Schematic representation of the problem.	24
2	Thermal transmittivity random field: (a) five samples, and (b) 10 largest-magnitude eigenvalues λ_i of the integral operator that has the covariance function (69) as its kernel.	25
3	Monte Carlo simulation: five samples of the neutron flux and temperature for (a,b) $k = 1$ J/K/cm/s, (c,d) $k = 10$ J/K/cm/s, and (e,f) $k = 100$ J/K/cm/s.	26
4	Elementary PC-based simulation: convergence of the nonlinear solver.	27
5	Elementary PC-based simulation: PC coordinates of (a) the random neutron flux and (b) the random temperature.	28
6	Elementary PC-based simulation: five samples of (a) the random neutron flux and (b) the random temperature.	29
7	Elementary PC-based simulation: convergence as a function of the order P	30
8	PC-based simulation with dimension reduction: convergence of the nonlinear solver.	31
9	PC-based simulation with dimension reduction: (a) mean, (b) eigenvalues λ_i , (c,d) eigenmodes φ_1^h and φ_2^h , and (e,f) PC coordinates of η_1^P and η_2^P for the KL decomposition of the temperature.	32
10	PC-based simulation with dimension reduction: (a) joint and (b,c) marginal probability density functions of η_1^P and η_2^P	33
11	PC-based simulation with dimension reduction: PC coordinates of (a) the random neutron flux and (b) the random temperature.	34
12	PC-based simulation with dimension reduction: five samples of (a) the random neutron flux and (b) the random temperature.	35
13	PC-based simulation with dimension reduction: convergence as a function of the order P of the PC expansions and the number n of terms retained in the KL decomposition.	36

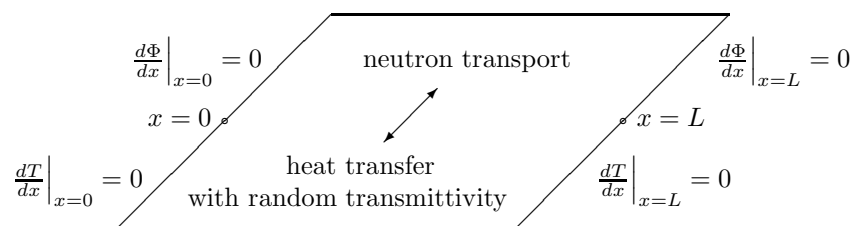


Figure 1. Schematic representation of the problem.

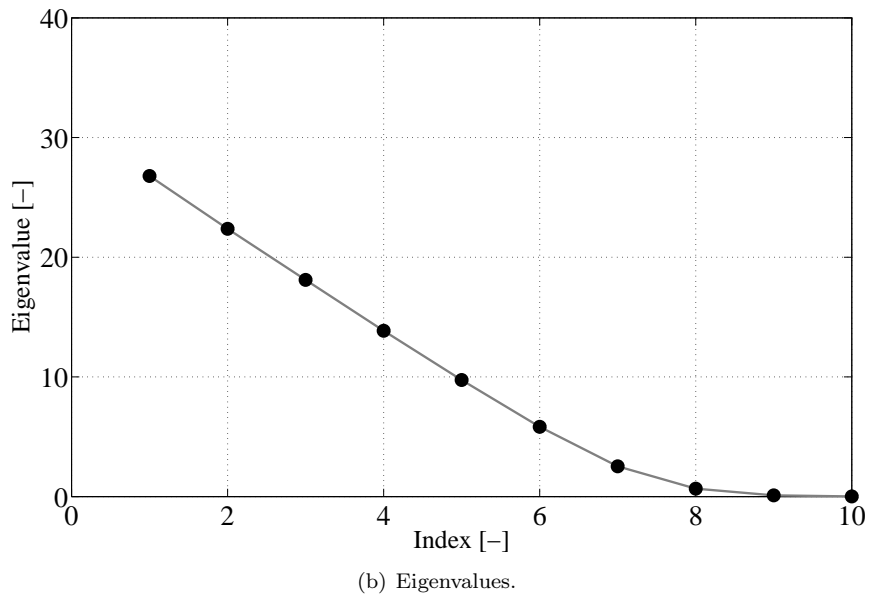
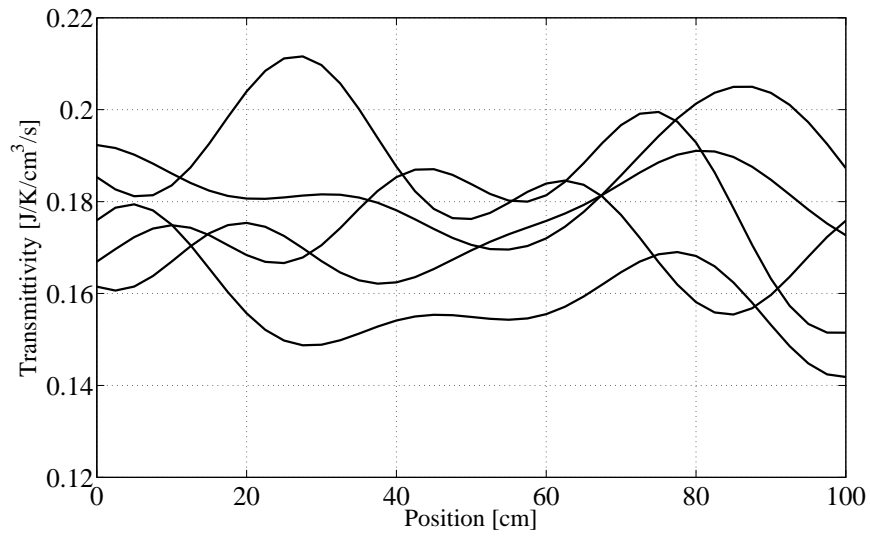


Figure 2. Thermal transmittivity random field: (a) five samples, and (b) 10 largest-magnitude eigenvalues λ_i of the integral operator that has the covariance function (69) as its kernel.

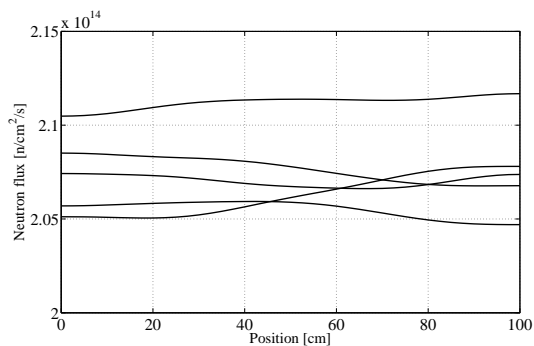
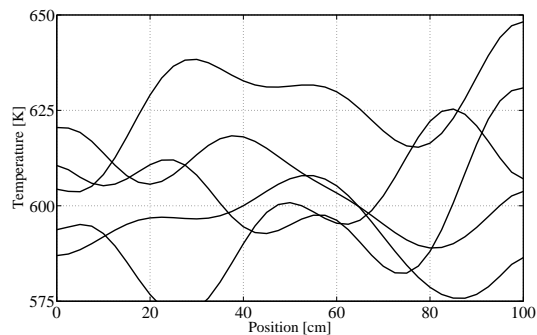
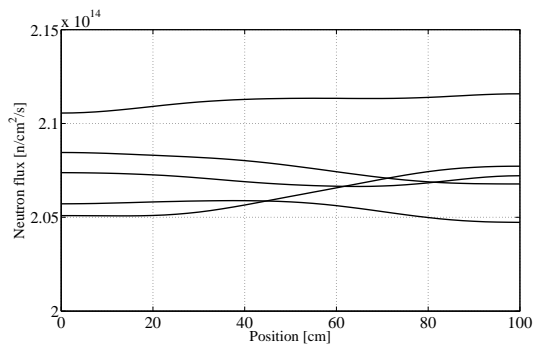
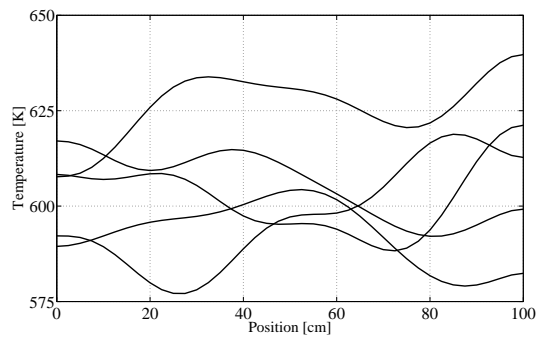
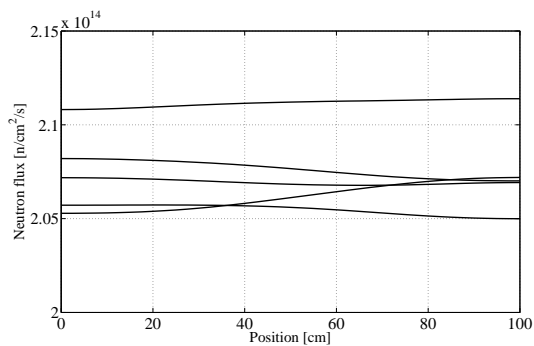
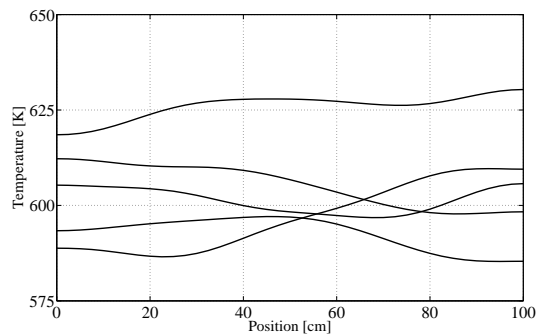
(a) Neutron flux for $k = 1 \text{ J/K/cm/s}$.(b) Temperature for $k = 1 \text{ J/K/cm/s}$.(c) Neutron flux for $k = 10 \text{ J/K/cm/s}$.(d) Temperature for $k = 10 \text{ J/K/cm/s}$.(e) Neutron flux for $k = 100 \text{ J/K/cm/s}$.(f) Temperature for $k = 100 \text{ J/K/cm/s}$.

Figure 3. Monte Carlo simulation: five samples of the neutron flux and temperature for (a,b) $k = 1 \text{ J/K/cm/s}$, (c,d) $k = 10 \text{ J/K/cm/s}$, and (e,f) $k = 100 \text{ J/K/cm/s}$.

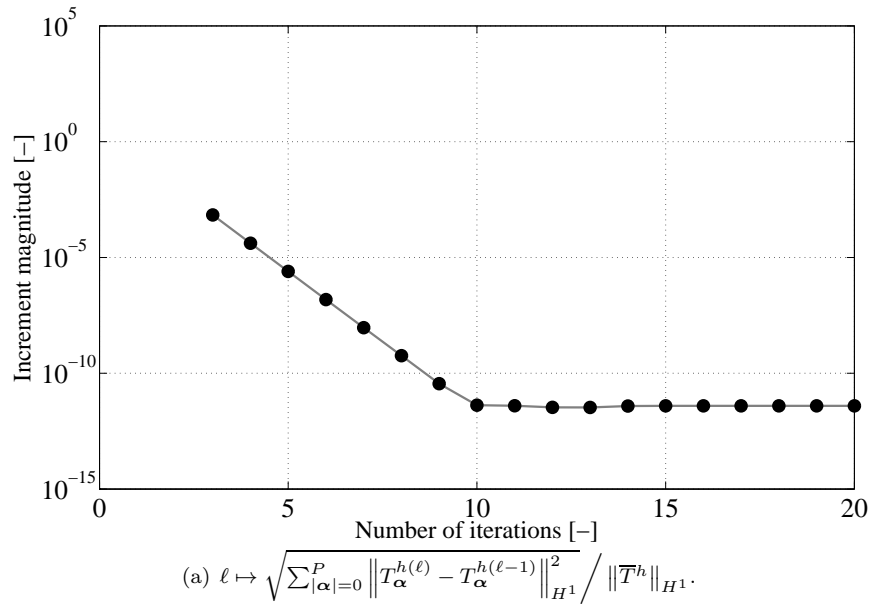
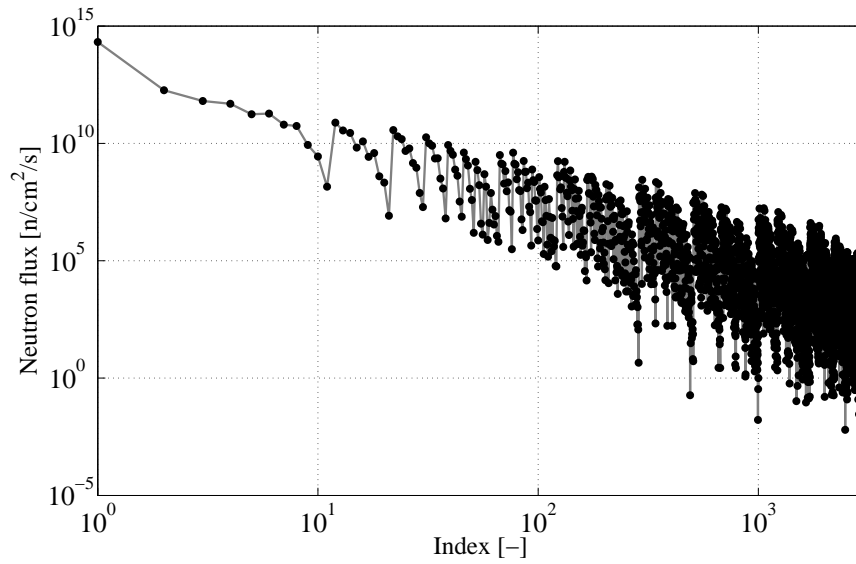
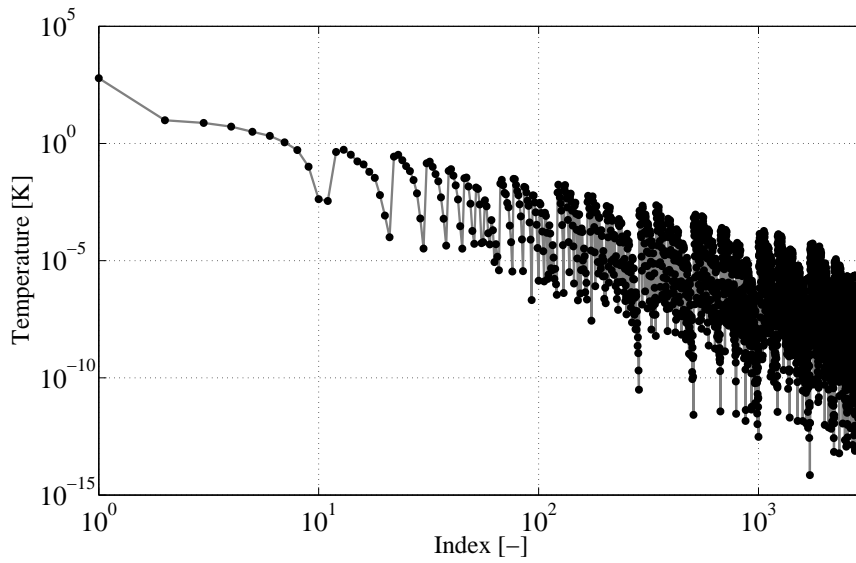


Figure 4. Elementary PC-based simulation: convergence of the nonlinear solver.

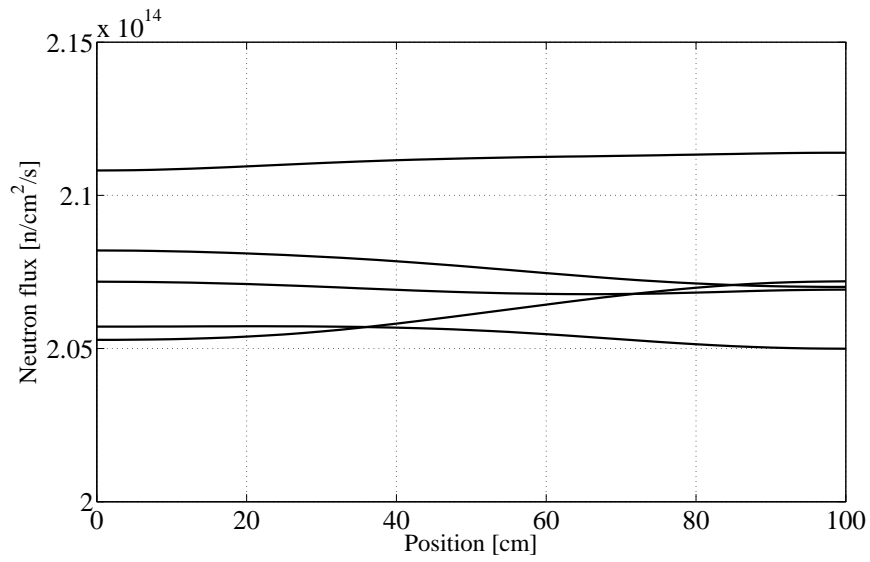


(a) Neutron flux.

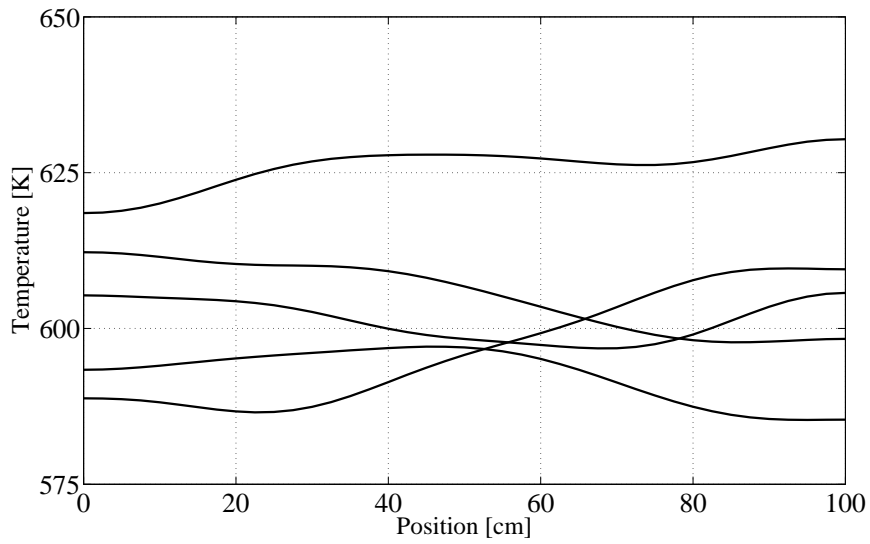


(b) Temperature.

Figure 5. Elementary PC-based simulation: PC coordinates of (a) the random neutron flux and (b) the random temperature.

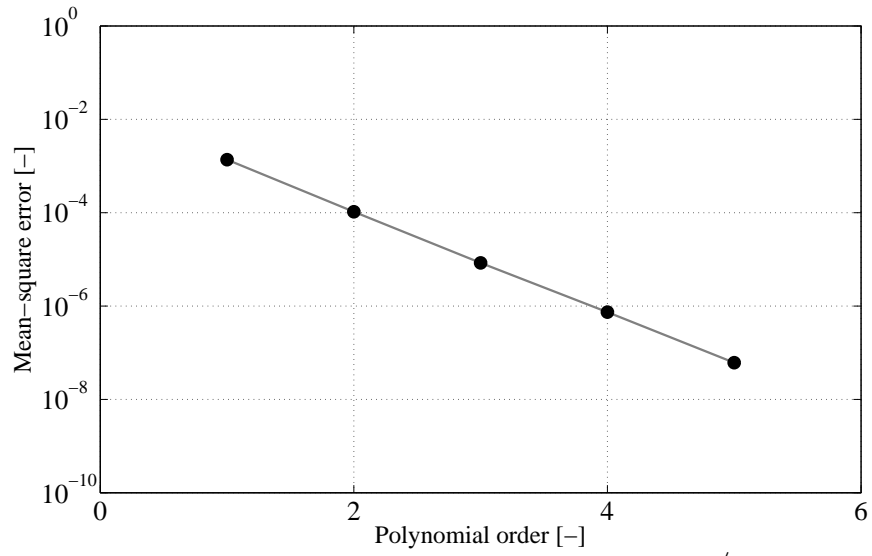


(a) Neutron flux.

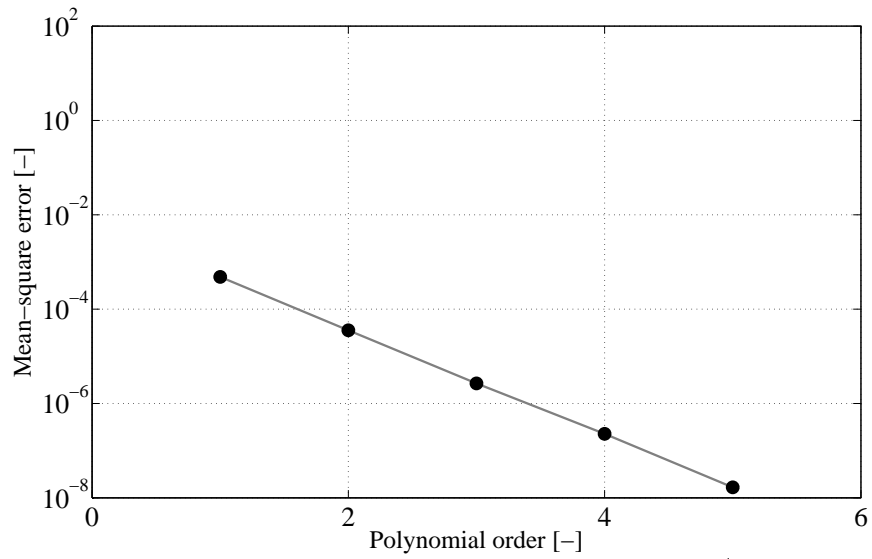


(b) Temperature.

Figure 6. Elementary PC-based simulation: five samples of (a) the random neutron flux and (b) the random temperature.



(a) $L^2 \otimes H^1$ -error estimate $\sqrt{\frac{1}{MC} \sum_{k=1}^{MC} \|\Phi^h(\xi_k) - \Phi^{hP}(\xi_k)\|_{H^1}^2} / \|\bar{\Phi}^h\|_{H^1}$.



(b) $L^2 \otimes H^1$ -error estimate $\sqrt{\frac{1}{MC} \sum_{k=1}^{MC} \|T^h(\xi_k) - T^{hP}(\xi_k)\|_{H^1}^2} / \|\bar{T}^h\|_{H^1}$.

Figure 7. Elementary PC-based simulation: convergence as a function of the order P .

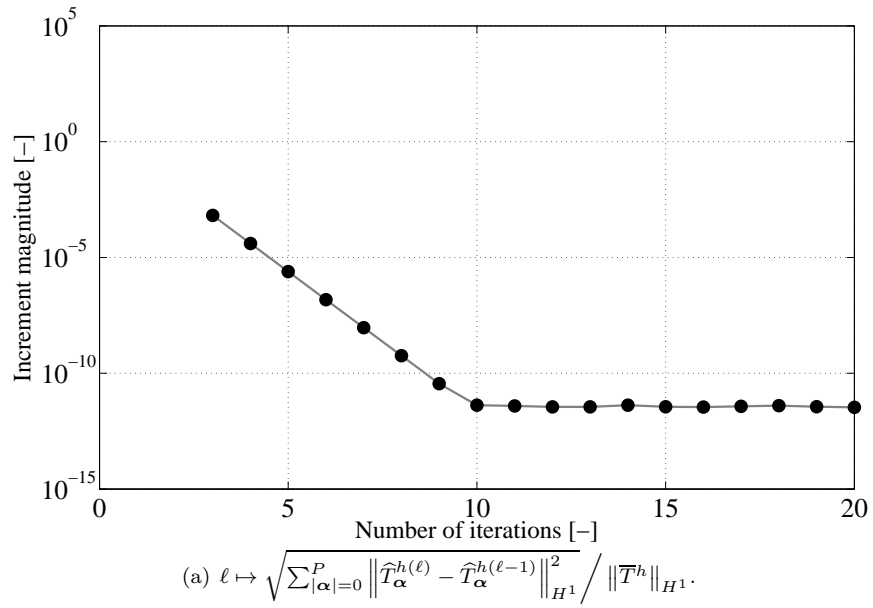


Figure 8. PC-based simulation with dimension reduction: convergence of the nonlinear solver.

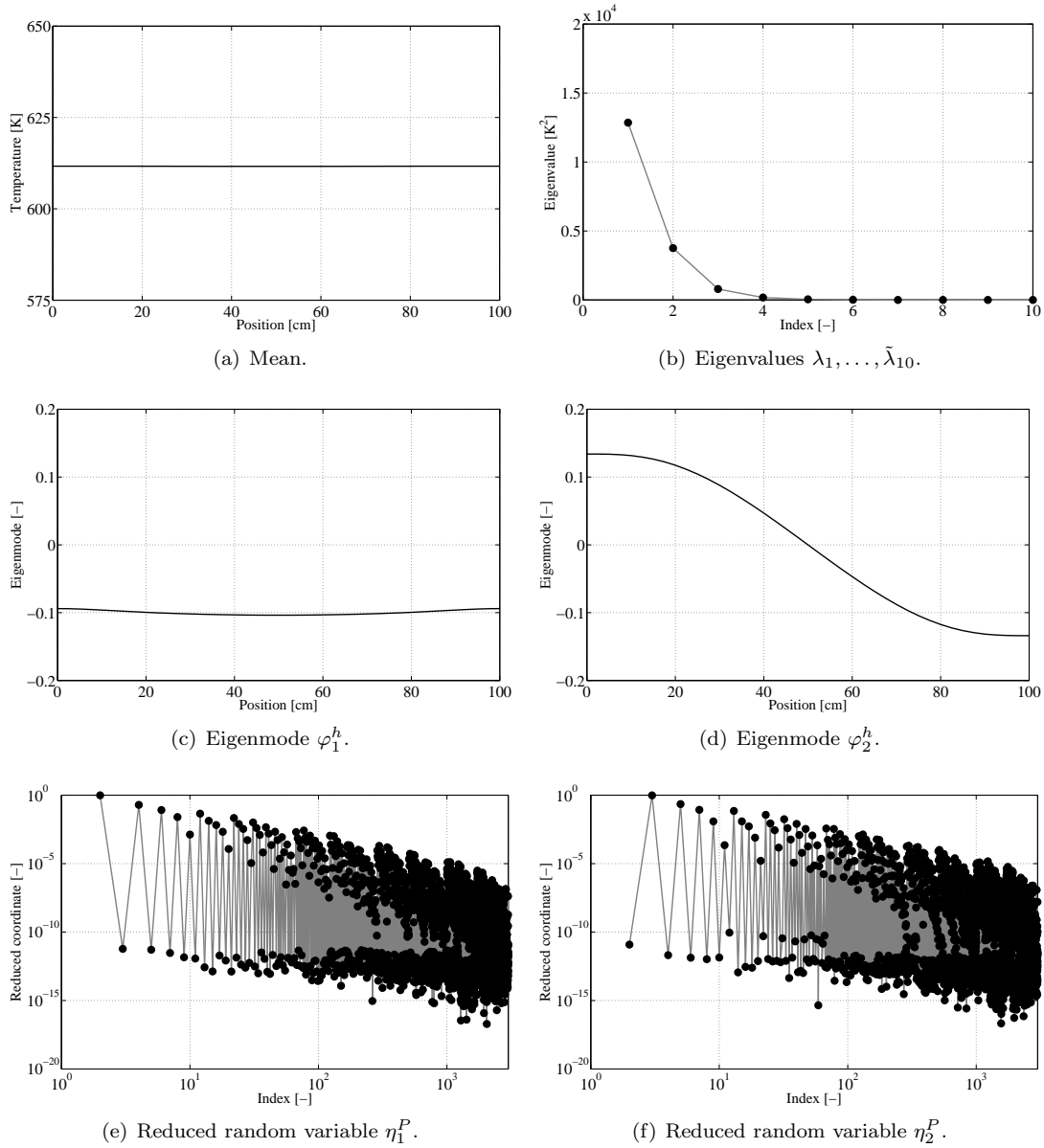
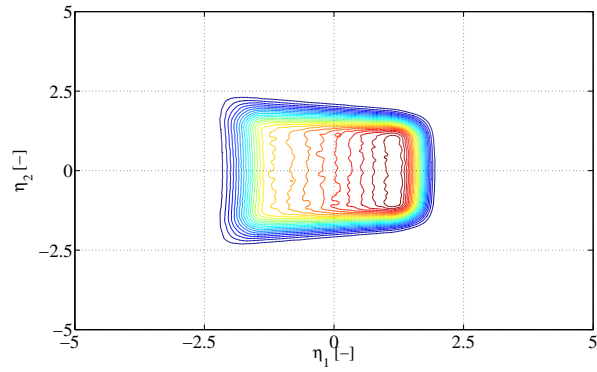
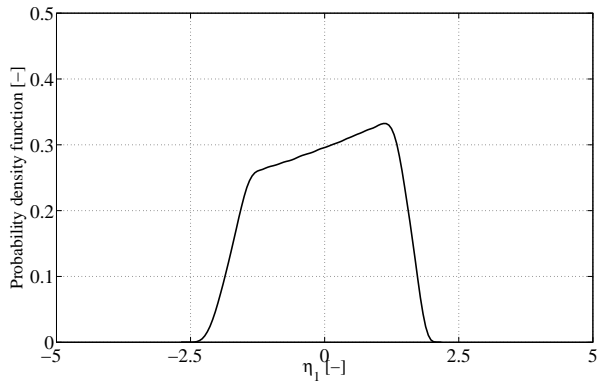


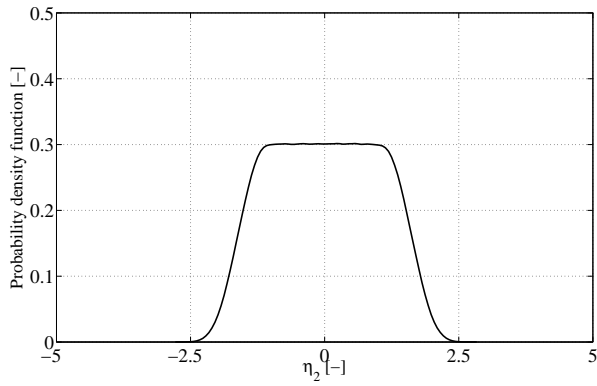
Figure 9. PC-based simulation with dimension reduction: (a) mean, (b) eigenvalues λ_i , (c,d) eigenmodes φ_1^h and φ_2^h , and (e,f) PC coordinates of η_1^P and η_2^P for the KL decomposition of the temperature.



(a) Joint probability density function of η_1^P and η_2^P .

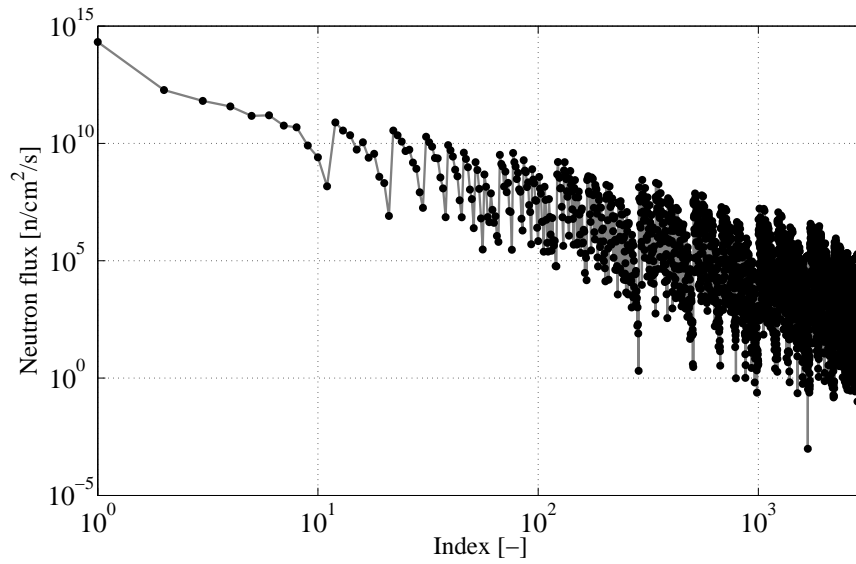


(b) Marginal probability density function of η_1^P .

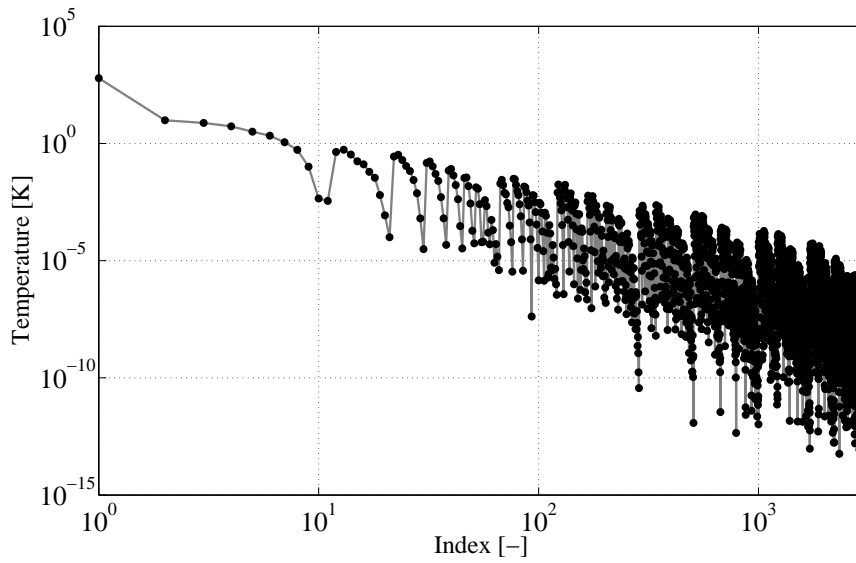


(c) Marginal probability density function of η_2^P .

Figure 10. PC-based simulation with dimension reduction: (a) joint and (b,c) marginal probability density functions of η_1^P and η_2^P .

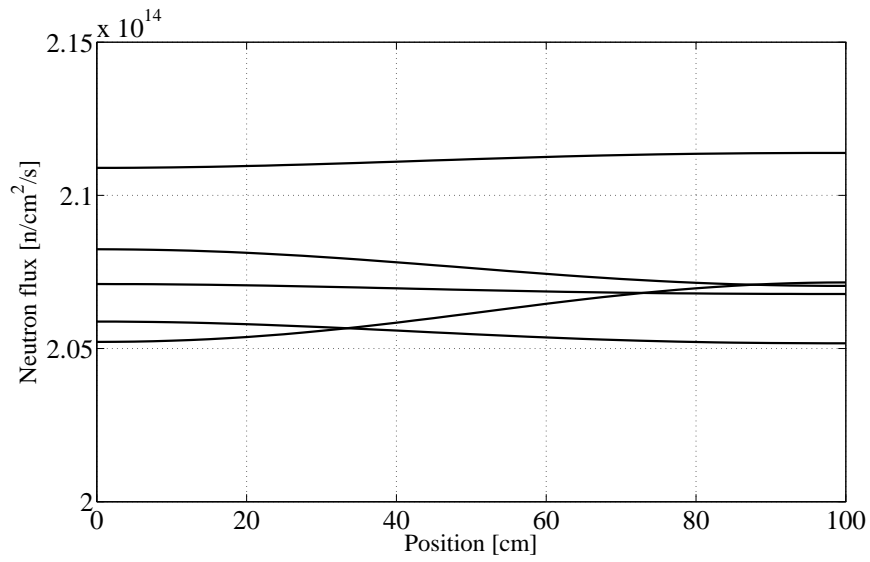


(a) Neutron flux.

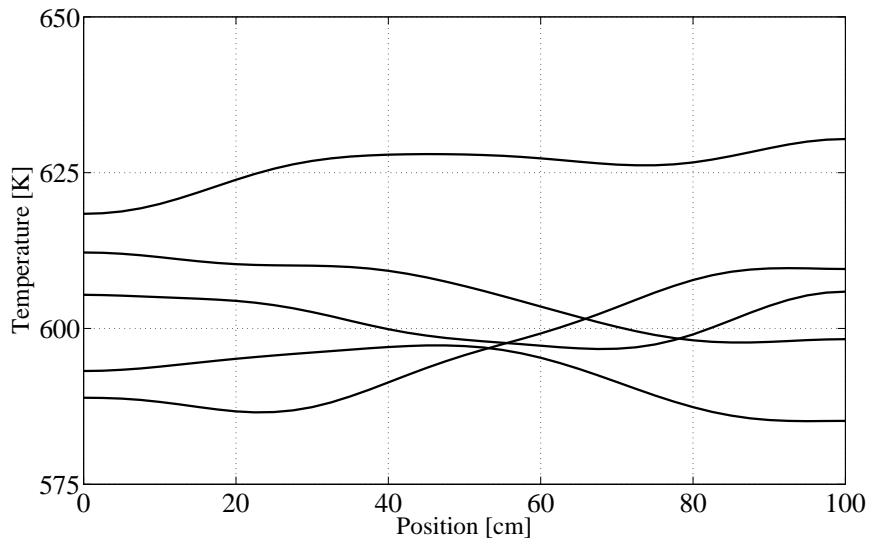


(b) Temperature.

Figure 11. PC-based simulation with dimension reduction: PC coordinates of (a) the random neutron flux and (b) the random temperature.

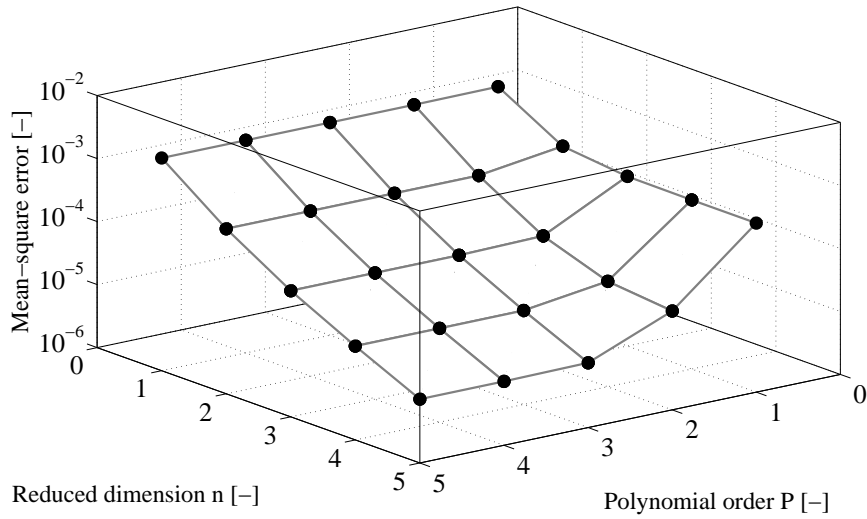


(a) Neutron flux.

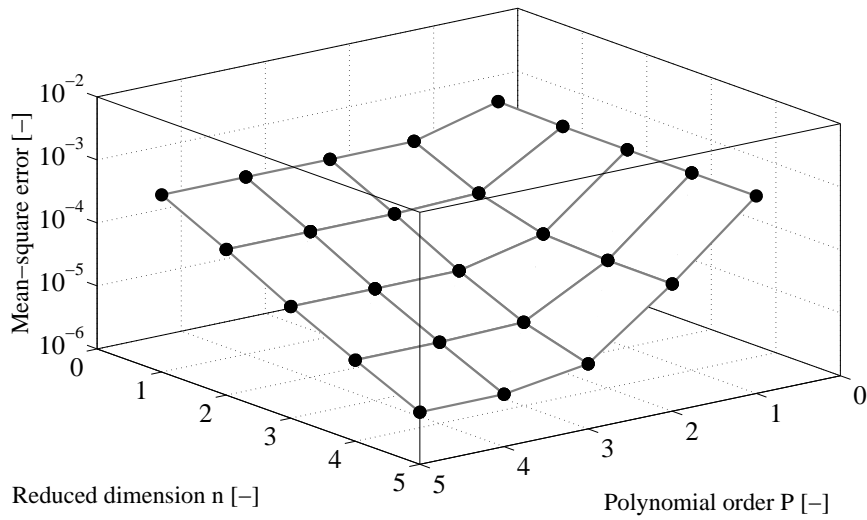


(b) Temperature.

Figure 12. PC-based simulation with dimension reduction: five samples of (a) the random neutron flux and (b) the random temperature.



(a) $L^2 \otimes H^1$ -error estimate $\sqrt{\frac{1}{MC} \sum_{k=1}^{MC} \|\Phi^h(\xi_k) - \hat{\Phi}^{hP}(\xi_k)\|_{H^1}^2} / \|\bar{\Phi}^h\|_{H^1}$.



(b) $L^2 \otimes H^1$ -error estimate $\sqrt{\frac{1}{MC} \sum_{k=1}^{MC} \|T^h(\xi_k) - \hat{T}^{hP}(\xi_k)\|_{H^1}^2} / \|\bar{T}^h\|_{H^1}$.

Figure 13. PC-based simulation with dimension reduction: convergence as a function of the order P of the PC expansions and the number n of terms retained in the KL decomposition.